Bioorg. Med. Chem. 131 (2025) 118419

Contents lists available at ScienceDirect

Bioorganic & Medicinal Chemistry

journal homepage: www.elsevier.com/locate/bmc

Exploring the potential of new acetylated unsaturated Oxindole derivatives as multi-target inhibitors for BACE1 and BuChE

Catarina A. Montargil [a,b,f], Mariana Pinto [a,b,f], Rosa Resende [b], Elisabete P. Carreiro [c], Alfonso T. García-Sosa [d], Armanda E. Santos [b,e], Anthony J. Burke [a,b,f,*]

[a] Laboratory of Pharmaceutical Chemistry, Faculty of Pharmacy, University of Coimbra, 3000-548 Coimbra, Portugal
[b] CNC-UC-Center for Neuroscience and Cell Biology, CIBB-Center for Innovative Biomedicine and Biotechnology, University Coimbra, Coimbra, Portugal
[c] LAQV-REQUIMTE, University of Évora, Institute of Research and Advanced Training (IIFA), 7000-671 Évora, Portugal
[d] Institute of Chemistry, University of Tartu, Ravila 14 A, Tartu 50411, Estonia
[e] Laboratory of Biochemistry and Biology, Faculty of Pharmacy, University of Coimbra, 3000-548 Coimbra, Portugal
[f] Coimbra Chemistry Centre – Institute of Molecular Sciences (CQC-IMS), Chemistry Department, University of Coimbra, 3004-535 Coimbra, Portugal

ARTICLE INFO

Keywords:
Alzheimer's disease
BACE1 activity
Cholinesterase
Oxindole derivatives
Molecular docking

ABSTRACT

Alzheimer's disease (AD) is the most common form of dementia worldwide, accounting for an estimated 60–70 % of cases. β-secretase 1 (BACE1), is one of the main therapeutic targets involved in the disease's pathology, as it is involved in the production of amyloid β. Butrylcholinesterase (BuChE) which is active in the advanced stages of the disease, is targeted for symptomatic relief. AD is a complex illness that needs to be tackled from different angles for which the Multi-target inhibitor approach is a viable current strategy. This work focuses on the development of novel acyl-oxindole molecules – some containing fluorine units, obtained via a structure-based drug design approach, for inhibition of BACE1 and BuChE. This study explored the development of a sustainable metal-based synthetic procedure for rapid and sustainable assess of libraries of these new oxindole derivatives. The compounds were screened to determine their ability to inhibit BACE1, and demonstrated reasonable levels of inhibition, with some of these inhibitors being selected for docking studies to determine the binding mode to the target's active site. One of the key molecules **12a** underwent a cytotoxicity screen in a mouse neuroblastoma cell line expressing the APPswe protein (N2A-APPswe cells) and was an inhibitor of both AChE and BuChE (more potent against the latter, including the human version). Some compounds (**3a**, **3b**, **3i** and **12a**) have shown moderate BuChE inhibitory activity.

1. Introduction

Alzheimer's disease (AD) is the most common form of dementia worldwide, accounting for an estimated 60–70 % of cases. It is characterized by a progressive decline in cognition, functional capacity, and behaviour, typically starting with recent memory loss. AD is a leading cause of disability morbidity in older adults and in the USA, it was the fifth-leading cause of death among individuals aged 65 and older in 2021. In addition to causing numerous deaths – according to the World Health Organization (WHO), around 1.6 million in 2019 – nearly 10 million new cases are reported annually. These numbers underscore the significant impact of the disease on people's lives, with dementia contributing far more to disability, care needs, and associated costs than other chronic, physical or mental illnesses.[1]

AD was first described by Alois Alzheimer in 1906 and is primarily associated with the abnormal accumulation of proteins, specifically amyloid β (Aβ) and Tau. The amyloid precursor protein (APP) is a transmembrane protein thought to be involved in neuronal growth and repair.[2,3] The proteolytic cleavage of APP occurs mainly via the non-amyloidogenic pathway, mediated by the sequential action of α- and γ-secretases, or the amyloidogenic pathway carried out by the sequential action of β- and γ-secretases. The metabolites generated in the amyloidogenic pathway include soluble APPβ (sAPPβ), β-amyloid (Aβ) peptides and the APP intracellular domain (AICD). The aggregation of Aβ peptide monomers ultimately leads to insoluble fibrils that accumulate to form extracellular deposits, the amyloid plaques. Soluble Aβ peptide oligomers and/or amyloid plaques hinder synaptic communication between neurons, thereby impairing brain functions, such as memory.[2,3]

* Corresponding author at: Laboratory of Pharmaceutical Chemistry, Faculty of Pharmacy, University of Coimbra, 3000-548 Coimbra, Portugal
E-mail address: ajburke@ff.uc.pt (A.J. Burke).

https://doi.org/10.1016/j.bmc.2025.118419
Received 29 March 2025; Received in revised form 23 September 2025; Accepted 24 September 2025
Available online 26 September 2025

β-Secretase (BACE-1) is the first protease to initiate the amyloid cascade (followed by the intervention of γ-Secretase) by cleaving the APP and is thus a therapeutic target for disease modification.[4] X-ray crystallography has shown that BACE-1 has a wide open active site with a flexible loop and some key residues for inhibitor binding, which include, Trp76, Asp32, Asp228, Thr231 etc., and most of the current therapeutic agents have been rationally designed to fit into this pocket (Fig. 1).[4,5] Many have already entered clinical trials (Fig. 1), and they generally have heterocyclic units in their core and on their periphery like; pyrimidines, picolinamides, dihydropyrimidinones, iminohydantoins etc,[6] but need-the-less to say that all phase II and III clinical trials were either concluded without benefit or discontinued owing to futility or the occurrence of adverse effects.[7] Thus there is a need for other structural motifs without these undesirable side-effects and downsides.

On the other hand, as regards AD progression there is a significant reduction in Acetylcholine (ACh) levels in the brain, worsening cognitive abilities. ACh is hydrolysed by cholinesterase enzymes, primarily by Acetylcholinesterase (AChE), although butyrlcholinesterase (BuChE) is also directly associated with this mechanism. Indeed, in advanced AD patients, the level of AChE in the brain decreases to approximately 55–67 %, whilst BuChE levels increase to around 120 %, suggesting that BuChE plays a significant role for these AD patients.[8–10] ChE inhibitors (like donepezil, rivastigmine, galantamine) competitively block AChE, and some also act on BuChE. These drugs only offer symptomatic relief and are not disease modifiers. In recent years, with a goal at obtaining multi-target inhibitors, our research group has developed several oxindole-based compounds that have been particularly selective against BuChE (Fig. 1).[11–13,15–19] In the case of complex diseases such as AD, with more than one protein target, the use of pleiotropic or multi-Targeting inhibitors, brings many significant advantages from the pharmacological and therapeutic point of view.[14] Thus in this article we discuss the development through sustainable synthetic routes of several novel acylated (including fluorine containing analogues) *N*-

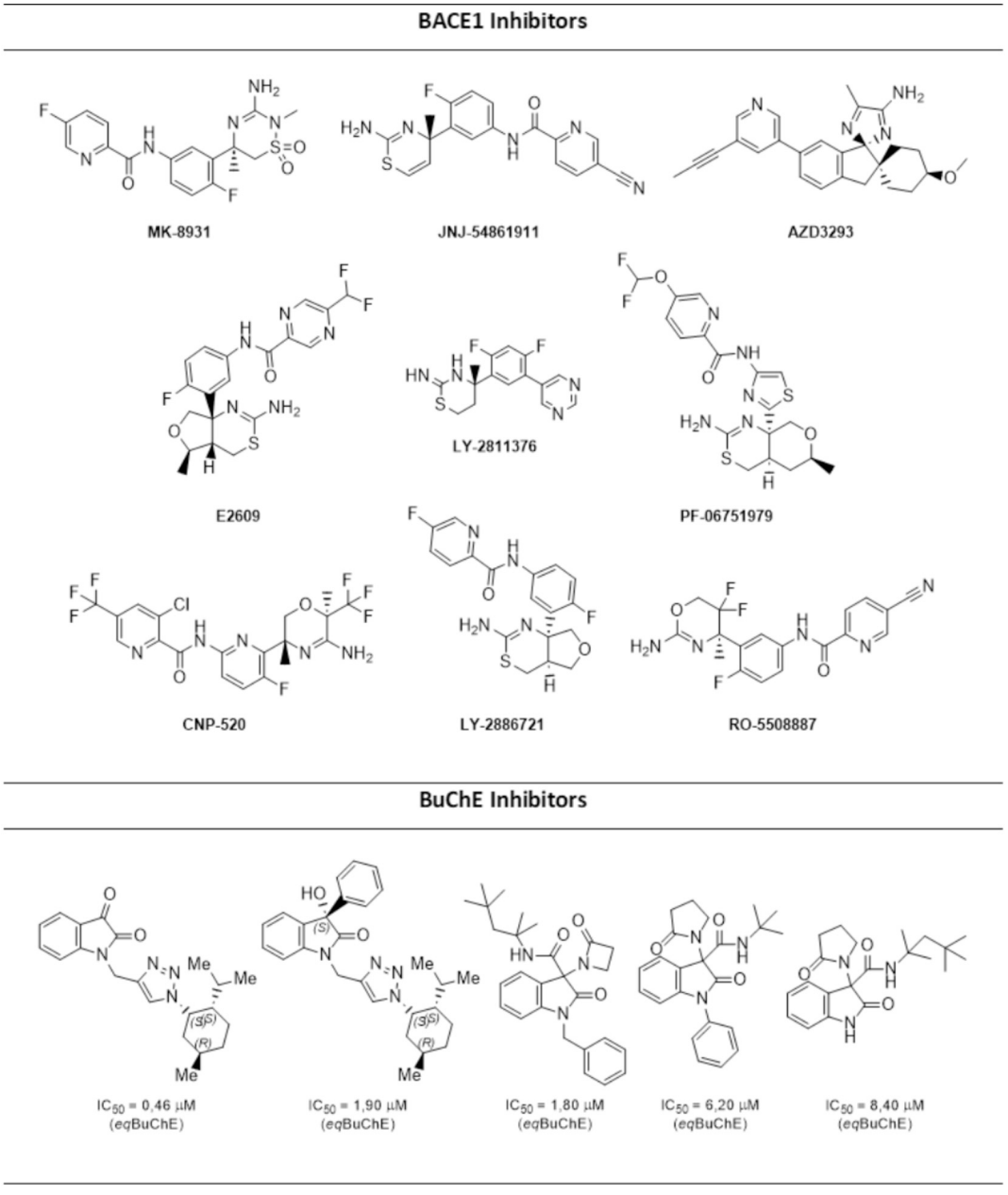

Fig. 1. Known BACE1 inhibitors, and some BuChE inhibitors reported by our group.

benzyl and *N*-allyl oxindoles.

2. Experimental

2.1. General

^{1}H NMR 400 MHz, ^{13}C APT NMR 101 MHz, and ^{19}F NMR 376 MHz spectra were run on a Bruker Avance III 400 MHz instrument in $CDCl_3$. A Thermo Orbitrap QExactive Focus was used to obtain mass spectra. Melting points were recorded on a Buchi B-540 apparatus in open capillary tubes. Reaction progress was screened by TLC using silica gel 60 F_{254} plates.

2.2. General procedure for the synthesis of compounds 2a-2i

Compounds **1a-1i** were prepared based on a procedure described in the literature. [15]

Starting from the corresponding isatin derivatives (6.80 mmol) in dry DMF (12 mL) at 0 °C, NaH (60 % dispersion in mineral oil, 7.20 mmol) was added under an inert atmosphere. When gas evolution stopped, allyl bromide (7.48 mmol) was slowly added. The reaction mixtures were stirred at room temperature for 5 h, and H_2O was added to precipitate the products. After filtration, the crude solids formed were washed with hexane to yield the pure products **1a-1i**.

Compounds **2a-2i** were prepared following a procedure described in the literature. [20]

Starting from the corresponding derivatives **1** (0.95 mmol) in DMF (3 mL), indium (0.95 mmol), sodium iodide (3.80 mmol), and allyl bromide (3.80 mmol) were added. The reaction mixtures were stirred at room temperature for 1 h, and hydrochloric acid (10 % aqueous solution) was added to end the reactions. After extraction with dichloromethane, the products were washed with brine and dried over anhydrous Na_2SO_4 to obtain the pure compounds **2a-2i**.

1-Allyl-4-bromoindoline-2,3-dione (1a). Orange powder, yield: 79 %, m.p: 133.8 °C; ^{1}H NMR (400 MHz, $CDCl_3$): $\delta = 7.38$ (t, $J = 8.0$ Hz, 1H), 7.25 (d, $J = 8.7$ Hz, 1H), 6.84 (d, $J = 7.7$ Hz, 1H), 5.88–5.77 (m, 1H), 5.34–5.28 (m, 2H), 4.38 (d, $J = 5.4$ Hz, 2H); ^{13}C APT NMR (101 MHz, $CDCl_3$): $\delta = 42.3$, 113.0, 117.3, 118.8, 122.0, 128.2, 131.4, 139.3, 148.2, 158.0, 181.4; Mass (ESI+) $m/z = 268.08$ $(M + H)^+$.

1-Allyl-5-bromoindoline-2,3-dione (1b). Red powder, yield: 82 %, m.p: 94.7 °C (literature: 93–95 °C) [21]; ^{1}H NMR (400 MHz, $CDCl_3$): $\delta = 7.73$ (s, 1H), 7.68 (d, $J = 8.3$ Hz, 1H), 6.80 (d, $J = 8.3$ Hz, 1H), 5.87–5.78 (m, 1H), 5.31 (dd, $J = 13.7$, 2.8 Hz, 2H), 4.36 (d, $J = 5.4$ Hz, 2H); ^{13}C APT NMR (101 MHz, $CDCl_3$): $\delta = 182.42$, 158.06, 149.81, 140.07, 131.53, 127.09, 119.91, 117.96, 115.39, 113.69, 42.19; Mass (ESI+) $m/z = 267.95$ $(M + H)^+$.

1-Allyl-5-chloroindoline-2,3-dione (1c). Red powder, yield: 85 %, m.p: 86.9 °C; ^{1}H NMR (400 MHz, $CDCl_3$): $\delta = 7.59$ (s, 1H), 7.53 (d, $J = 10.7$ Hz, 1H), 6.85 (d, $J = 8.5$ Hz, 1H), 5.89–5.75 (m, 1H), 5.32 (m, 2H), 4.37 (d, $J = 5.4$ Hz, 2H).; ^{13}C APT NMR (101 MHz, $CDCl_3$): $\delta = 182.57$, 158.22, 149.44, 137.25, 131.56, 127.86, 124.36, 119.53, 117.98, 113.24, 42.21; Mass (ESI+) $m/z = 222.01$ $(M + H)^+$.

1-Allyl-5-nitroindoline-2,3-dione (1d). Orange powder, yield: 75 %, m.p: 120.6–121.0 °C; ^{1}H NMR (400 MHz, $CDCl_3$): $\delta = 8.51$ (dddd, $J = 8.6$, 2.4 Hz, 2H), 7.05 (d, $J = 8.6$ Hz, 1H), 5.93–5.77 (m, 1H), 5.36 (m, 2H), 4.46 (d, $J = 5.4$ Hz, 2H); ^{13}C APT NMR (101 MHz, $CDCl_3$): $\delta = 181.07$, 157.53, 154.86, 144.20, 133.54, 129.39, 121.02, 119.65, 117.21, 111.15, 43.03; Mass (ESI+) m/z = 233.07 $(M + H)^+$.

1-Allyl-5-fluroindoline-2,3-dione (1e). Red powder, yield: 72 %, m.p: 79.4–79.8 °C; ^{1}H NMR (400 MHz, $CDCl_3$): $\delta = 7.57$–7.46 (m, 2H), 7.08 (dd, $J = 8.6$, 3.9 Hz, 1H), 5.90–5.80 (m, 1H), 5.36 (d, $J = 18.8$ Hz, 1H), 5.20 (d, $J = 10.4$ Hz, 1H), 4.32 (d, $J = 5.0$ Hz, 2H); ^{13}C APT NMR (101 MHz, $CDCl_3$): $\delta = 183.08$, 160.14, 157.74, 147.16, 131.66, 124.44, 117.98, 117.38, 112.96, 111.75, 42.19; ^{19}F NMR (376 MHz, $CDCl_3$): $\delta = -120.24$; Mass (ESI+) $m/z = 206.29$ $(M + H)^+$.

1-Allyl-5-methoxyindoline-2,3-dione (1f). Red-brown powder, yield: 76 %, m.p: 91.1–92.1 °C; ^{1}H NMR (400 MHz, $CDCl_3$): $\delta = 7.34$ (d, $J = 8.6$ Hz, 1H), 7.25 (s, 1H), 7.10 (d, $J = 8.6$ Hz, 1H), 6.00–5.87 (m, 1H), 5.42 (d, $J = 17.2$ Hz, 1H), 5.29 (d, $J = 9.0$ Hz, 1H), 4.39 (d, $J = 5.0$ Hz, 2H), 3.87 (s, 3H); ^{13}C APT NMR (101 MHz, $CDCl_3$): $\delta = 183.94$, 158.42, 156.19, 131.90, 124.28, 118.51, 117.85, 112.64, 109.62, 56.35, 42.13; Mass (ESI+) $m/z = 218.30$ $(M + H)^+$.

1-Allyl-5-(trifluoromethoxy)indoline-2,3-dione (1 g). Orange oil, yield: 68 %; ^{1}H NMR (400 MHz, $CDCl_3$): $\delta = 7.48$ (s, 1H), 7.43 (d, $J = 8.5$ Hz, 1H), 6.93 (d, $J = 8.6$ Hz, 1H), 5.90–5.75 (m, 1H), 5.33 (m, 2H), 4.38 (d, $J = 5.4$ Hz, 2H); ^{13}C APT NMR (101 MHz, $CDCl_3$): $\delta = 182.27$, 157.62, 149.15, 145.33, 129.92, 121.65, 119.13, 118.50, 118.06, 113.75, 112.10, 42.73; ^{19}F NMR (376 MHz, $CDCl_3$): $\delta = -58.64$; Mass (ESI+) $m/z = 272.29$ $(M + H)^+$.

1-Allyl-4,7-dichloroindoline-2,3-dione (1 h). Orange powder, yield: 90 %, m.p: 160.8–161.8 °C; ^{1}H NMR (400 MHz, $CDCl_3$): $\delta = 7.42$ (d, $J = 8.7$ Hz, 1H), 7.02 (d, $J = 8.7$ Hz, 1H), 6.04–5.87 (m, 1H), 5.24 (m, 2H), 4.77 (d, $J = 5.0$ Hz, 2H); ^{13}C APT NMR (101 MHz, $CDCl_3$): $\delta = 179.33$, 157.50, 147.16, 140.56, 132.98, 131.56, 126.38, 117.83, 116.84, 115.54, 43.72; Mass (ESI+) $m/z = 256.07$ $(M + H)^+$.

1-Allyl-7-(trifluoromethyl)indoline-2,3-diona (1i). Orange powder, yield: 96 %, m.p: 72.9–73.4 °C; ^{1}H NMR (400 MHz, $CDCl_3$): $\delta = 7.85$ (dd, $J = 17.1$, 8.6 Hz, 2H), 7.23 (d, $J = 7.3$ Hz, 1H), 5.94–5.78 (m, 1H), 5.21 (dd, $J = 12.8$, 1.6 Hz, 2H), 4.58 (d, $J = 5.0$ Hz, 2H); ^{13}C APT NMR (101 MHz, $CDCl_3$): $\delta = 181.67$, 158.87, 135.76, 130.46, 128.90, 123.97, 123.47, 121.27, 120.04, 117.70, 114.51, 44.69; ^{19}F NMR (376 MHz, $CDCl_3$): $\delta = -55.88$; Mass (ESI+) m/z = 256.14 $(M + H)^+$.

1,3-Diallyl-4-bromo-3-hydroxyindolin-2-one (2a). Yellow oil, yield: 82 %; ^{1}H NMR (400 MHz, $CDCl_3$): $\delta = 7.19$ (d, $J = 7.1$ Hz, 1H), 7.13 (t, $J = 8.0$ Hz, 1H), 6.73 (d, $J = 7.6$ Hz, 1H), 5.83–5.69 (m, 1H), 5.43–5.30 (m, 1H), 5.20 (dd, $J = 12.1$, 2.3 Hz, 2H), 5.10 (d, $J = 17.0$ Hz, 1H), 4.95 (d, $J = 10.0$ Hz, 1H), 4.42 (dd, $J = 16.6$, 5.0 Hz, 1H), 4.15 (dd, $J = 16.5$, 5.3 Hz, 1H), 3.25 (dd, $J = 12.8$, 6.7 Hz, 1H), 2.83 (dd, $J = 8.3$, 4.5 Hz, 1H); ^{13}C APT NMR (101 MHz, $CDCl_3$): $\delta = 176.21$, 144.69, 130.95, 130.68, 129.91, 127.38, 127.10, 120.50, 119.37, 117.92, 108.38, 77.76, 42.43, 40.16; Mass (ESI+) $m/z = 308.18$ $(M + H)^+$.

1,3-Diallyl-5-bromo-3-hydroxyindolin-2-one (2b). Yellow oil, yield: 81 %; ^{1}H NMR (400 MHz, $CDCl_3$): $\delta = 7.50$ (s, 1H), 7.41 (d, $J = 8.3$ Hz, 1H), 6.69 (d, $J = 8.3$ Hz, 1H), 5.82–5.72 (m, 1H), 5.68–5.53 (m, 1H), 5.24–5.09 (m, 4H), 4.39 (ddt, $J = 16.5$, 5.1, 1.8 Hz, 1H), 4.16 (ddt, $J = 16.4$, 5.4, 1.6 Hz, 1H), 2.74 (dd, $J = 13.4$, 6.3 Hz, 1H), 2.62 (dd, $J = 13.3$, 8.4 Hz, 1H·^{13}C APT NMR (101 MHz, $CDCl_3$): $\delta = 176.87$, 141.54, 132.40, 131.64, 130.71, 129.92, 127.45, 121.07, 117.92, 115.74, 110.85, 75.74, 42.96, 42.39; Mass (ESI+) $m/z = 310.13$ $(M + H)^+$.

1,3-Diallyl-5-chloro-3-hydroxyindolin-2-one (2c). Yellow oil, yield: 95 %; ^{1}H NMR (400 MHz, $CDCl_3$): $\delta = 8.23$ (s, 1H), 8.19 (d, $J = 8.6$ Hz, 1H), 6.84 (d, $J = 8.6$ Hz, 1H), 5.78–5.69 (m, 1H), 5.57–5.46 (m, 1H), 5.18 (m, 2H), 5.03 (m, 2H), 4.39 (dd, $J = 16.6$, 3.3 Hz, 1H), 4.21 (dd, $J = 17.4$, 4.4 Hz, 1H), 2.77–2.59 (m, 2H); ^{13}C APT NMR (101 MHz, $CDCl_3$): $\delta = 207.01$, 162.56, 131.50, 130.80, 130.08, 129.35, 128.23, 124.65, 120.81, 117.80, 110.28, 75.77, 42.88, 42.35; Mass (ESI+) $m/z = 286.12$ $(M + Na)^+$.

1,3-Diallyl-5-nitro-3-hydroxyindolin-2-one (2d). Yellow oil, yield: 90 %; ^{1}H NMR (400 MHz, $CDCl_3$): $\delta = 7.12$ (d, $J = 7.7$ Hz, 1H), 6.95 (t, 1H), 6.71 (dd, $J = 8.5$, 4.0 Hz, 1H), 5.83–5.66 (m, 1H), 5.63–5.45 (m, 1H), 5.19 (m, 2H), 5.05 (m, 2H), 4.37 (dd, $J = 16.4$, 5.0 Hz, 1H), 4.14 (dd, $J = 16.4$, 5.4 Hz, 1H), 2.78–2.58 (m, 2H); ^{13}C APT NMR (101 MHz, $CDCl_3$): $\delta = 177.59$, 162.75, 148.21, 143.54, 130.27, 129.70, 126.39, 121.11, 120.05, 118.24, 108.85, 75.43, 42.98, 42.53; Mass (ESI+) $m/z = 275.18$ $(M + H)^+$.

1,3-Diallyl-5-fluoro-3-hydroxyindolin-2-one (2e). Orange oil, yield: 99 %; ^{1}H NMR (400 MHz, $CDCl_3$): $\delta = 7.00$ (s, 1H), 6.82–6.66 (m, 2H), 5.86–5.70 (m, 1H), 5.67–5.50 (m, 1H), 5.25–5.15 (m, 2H), 5.13–5.03 (m, 2H), 4.25 (ddd, $J = 92.9$, 16.4, 5.2 Hz, 2H), 2.77–2.60 (m, 2H); ^{13}C APT NMR (101 MHz, $CDCl_3$): $\delta = 177.55$, 160.59, 158.19, 138.27, 131.57, 130.92, 130.13, 120.68, 117.80, 115.77, 112.46,

109.93, 76.14, 42.90, 42.44; ^{19}F NMR (376 MHz, $CDCl_3$): $\delta = -120.90$; Mass (ESI+) $m/z = 248.09$ $(M + H)^+$.

1,3-Diallyl-5-methoxy-3-hydroxyindolin-2-one (2f). Red-brown oil, yield: 89 %; ^{1}H NMR (400 MHz, $CDCl_3$): $\delta = 7.10$ (d, $J = 8.7$ Hz, 1H), 6.89 (d, $J = 8.7$ Hz, 1H), 5.92–5.75 (m, 1H), 5.38–5.22 (m, 1H), 5.13–4.88 (m, 4H), 4.68–4.55 (m, 2H), 3.13 (dd, $J = 13.8$, 7.0 Hz, 1H), 2.80 (dd, 1H); ^{13}C APT NMR (101 MHz, $CDCl_3$): $\delta = 177.22$, 156.22, 135.78, 131.27, 130.98, 130.52, 120.44, 117.57, 114.08, 111.17, 109.80, 76.17, 55.83, 43.06, 42.38; Mass (ESI+) $m/z = 260.03$ $(M + H)^+$.

1,3-Diallyl-5-trifluoromethoxy-3-hydroxyindolin-2-one (2 g). Orange oil, yield: 87 %; ^{1}H NMR (400 MHz, $CDCl_3$): $\delta = 7.28$ (s, 1H), 7.14 (d, $J = 8.5$ Hz, 1H), 6.79 (d, $J = 8.5$ Hz, 1H), 5.88–5.70 (m, 1H), 5.70–5.50 (m, 1H), 5.28–5.16 (m, 2H), 5.16–5.04 (m, 2H), 4.40 (m, 1H), 4.18 (m, 1H), 2.79–2.59 (m, 2H); ^{13}C APT NMR (101 MHz, $CDCl_3$): $\delta = 177.44$, 144.97, 141.04, 131.30, 130.74, 129.90, 122.54, 121.80, 120.95, 118.24, 118.01, 109.83, 75.89, 42.92, 42.47; ^{19}F NMR (376 MHz, $CDCl_3$): $\delta = -58.37$; Mass (ESI+) $m/z = 314.15$ $(M + H)^+$.

1,3-Diallyl-4,7-dichloro-3-hydroxyindolin-2-one (2 h). Orange oil, yield: 97 %; ^{1}H NMR (400 MHz, $CDCl_3$): $\delta = 7.05$ (dd, $J = 84.3$, 8.7 Hz, 2H), 5.96–5.79 (m, 1H), 5.43–5.27 (m, 1H), 5.18–4.96 (m, 4H), 4.71–4.59 (m, 2H), 3.18 (dd, $J = 13.6$, 6.4 Hz, 1H), 2.85 (m, 1H); ^{13}C APT NMR (101 MHz, $CDCl_3$): $\delta = 176.85$, 140.31, 133.06, 132.44, 130.23, 129.63, 128.32, 124.91, 120.87, 116.80, 114.20, 76.67, 43.49, 40.16; Mass (ESI+) $m/z = 298.12$ $(M + H)^+$.

1,3-Diallyl-7-trifluoromethyl-3-hydroxyindolin-2-one (2i). Orange oil, yield: 92 %; ^{1}H NMR (400 MHz, $CDCl_3$): $\delta = 7.63$–7.54 (m, 2H), 7.17 (t, $J = 7.8$ Hz, 1H), 5.95–5.71 (m, 1H), 5.69–5.48 (m, 1H), 5.14–5.04 (m, 4H), 4.55–4.45 (m, 2H), 2.77–2.60 (m, 2H); ^{13}C APT NMR (101 MHz, $CDCl_3$): $\delta = 178.90$, 163.27, 132.57, 131.38, 129.75, 127.80, 127.52, 124.70, 122.51, 121.12, 116.53, 73.78, 44.13, 43.26; ^{19}F NMR (376 MHz, $CDCl_3$): $\delta = -55.25$; Mass (ESI+) m/z = 256.14 $(M + H)^+$.

2.3. General procedure for the synthesis of compounds 3a-3i

Compounds **3a-3i** were prepared according to a procedure described in the literature.[22]

To the corresponding derivatives **2** (0.16 mmol), acetic anhydride (8 mmol) and potassium acetate (catalytic amount) were added. The reaction mixtures were stirred at 70 °C for 3 h. After extraction with dichloromethane, the products were washed with sodium bicarbonate and dried over anhydrous Na_2SO_4 to obtain the pure compounds **3a-3i**.

1,3-Diallyl-4-bromo-2-oxoindolin-3-yl acetate (3a). Yellow oil, yield: 88 %; ^{1}H NMR (400 MHz, $CDCl_3$): $\delta = 7.20$–7.06 (m, 2H), 6.73 (d, $J = 8.7$ Hz, 1H), 5.83–5.72 (m, 1H), 5.36–5.29 (m, 1H), 5.28–5.18 (m, 2H), 5.09–4.92 (m, 2H), 4.37–4.24 (m, 2H), 3.24 (dd, $J = 14.3$, 6.9 Hz, 1H), 2.83 (m, 1H), 2.09 (s, 3H); ^{13}C APT NMR (101 MHz, $CDCl_3$): $\delta = 173.18$, 169.02, 145.01, 130.86, 128.56, 126.56, 125.14, 121.91, 120.92, 118.82, 117.77, 108.26, 80.45, 42.53, 37.85, 20.13; HRESIMS: calcd for $(M + Na)^+$, 372.0211; found, 372.0201.

1,3-Diallyl-5-bromo-2-oxoindolin-3-yl acetate (3b). Orange oil, yield: 88 %; ^{1}H NMR (400 MHz, $CDCl_3$): $\delta = 7.58$–7.30 (m, 2H), 6.69 (d, $J = 8.3$ Hz, 1H), 5.84–5.74 (m, 1H), 5.63–5.45 (m, 1H), 5.33–5.21 (m, 2H), 5.13–5.03 (m, 2H), 4.36–4.30 (m, 2H), 2.81 (m, 1H), 2.59 (dd, $J = 13.5$, 8.2 Hz, 1H), 2.07 (s, 3H); ^{13}C APT NMR (101 MHz, $CDCl_3$): $\delta = 173.51$, 168.91, 142.01, 132.37, 130.77, 129.19, 128.80, 126.08, 121.25, 117.86, 115.14, 110.83, 77.34, 42.55, 40.81, 20.55; HRESIMS: calcd for $(M + Na)^+$, 372.0211; found, 372.0204.

1,3-Diallyl-5-chloro-2-oxoindolin-3-yl acetate (3c). Orange oil, yield: 52 %; ^{1}H NMR (400 MHz, $CDCl_3$): $\delta = 7.26$–7.16 (m, 2H), 6.74 (d, $J = 8.3$ Hz, 1H), 5.86–5.73 (m, 1H), 5.61–5.48 (m, 1H), 5.33–5.20 (m, 2H), 5.13–5.04 (m, 2H), 4.37–4.27 (m, 2H), 2.81 (dd, $J = 13.5$, 6.3 Hz, 1H), 2.59 (dd, $J = 14.4$, 8.2 Hz, 1H), 2.07 (s, 3H); ^{13}C APT NMR (101 MHz, $CDCl_3$): $\delta = 173.63$, 168.90, 141.51, 130.82, 129.46, 128.85, 127,90, 123.36, 121.22, 117.96, 117.86, 110.33, 79.04, 42.58, 40.81, 20.54; HRESIMS: calcd for $(M + Na)^+$, 328.0716; found, 328.0705.

1,3-Diallyl-5-nitro-2-oxoindolin-3-yl acetate (3d). Brown oil, yield: 52 %; ^{1}H NMR (400 MHz, $CDCl_3$): $\delta = 8.26$ (d, $J = 8.7$ Hz, 1H), 8.11 (s, 1H), 6.90 (d, $J = 8.7$ Hz, 1H), 5.88–5.71 (m, 1H), 5.64–5.45 (m, 1H), 5.36–5.26 (m, 2H), 5.15–5.04 (m, 2H), 4.47–4.33 (m, 2H), 2.87 (dd, $J = 13.6$, 6.4 Hz, 1H), 2.63 (dd, 1H), 2.10 (s, 3H); ^{13}C APT NMR (101 MHz, $CDCl_3$): $\delta = 174.14$, 169.14, 148.53, 143.28, 130.14, 128.47, 128.22, 126.67, 121.93, 118.84, 118.45, 108.97, 78.36, 42.83, 40.62, 20.43; HRESIMS: calcd for $(M + Na)^+$, 339.0957; found, 339.0950.

1,3-Diallyl-5-fluro-2-oxoindolin-3-yl acetate (3e). Orange oil, yield: 69 %; ^{1}H NMR (400 MHz, $CDCl_3$): $\delta = 7.00$–6.93 (m, 2H), 6.73 (dd, $J = 9.2$, 4.0 Hz, 1H), 5.81 (ddd, $J = 22.3$, 10.3, 5.1 Hz, 1H), 5.61–5.49 (m, 1H), 5.35–5.20 (m, 2H), 5.11–5.04 (m, 2H), 4.32 (dd, $J = 5.2$, 1.6 Hz, 2H), 2.81 (dd, $J = 13.5$, 6.3 Hz, 1H), 2.58 (dd, $J = 13.5$, 8.1 Hz, 1H), 2.07 (s, 3H); ^{13}C APT NMR (101 MHz, $CDCl_3$): $\delta = 20.4$, 40.7, 42.6, 79.8, 110.0, 117.9, 119.4, 122.2, 126.9, 128.5, 129.4, 130.8, 139.0, 141.8, 168.9, 173.6; ^{19}F NMR (376 MHz, $CDCl_3$): $\delta = 120.41$. HRESIMS: calcd for $(M + Na)^+$, 312.1012; found, 312.1003.

1,3-Diallyl-5-methoxy-2-oxoindolin-3-yl acetate (3f). Brown oil, yield: 86 %; ^{1}H NMR (400 MHz, $CDCl_3$): $\delta = 6.86$–6.67 (m, 3H), 5.89–5.76 (m, 1H), 5.65–5.45 (m, 1H), 5.34–5.20 (m, 2H), 5.13–5.04 (m, 2H), 4.32 (d, $J = 1.7$ Hz, 2H), 3.77 (s, 3H), 2.80 (m, 1H), 2.60 (dd, $J = 13.4$, 8.2 Hz, 1H), 2.06 (s, 3H); ^{13}C APT NMR (101 MHz, $CDCl_3$): $\delta = 168.86$, 155.80, 136.37, 131.33, 129.35, 128.48, 120.75, 117.55, 113.39, 111.22, 110.60, 109.69, 79.60, 55.76, 42.57, 40.98, 20.64; HRESIMS: calcd for $(M + Na)^+$, 324.1212; found, 324.1203.

1,3-Diallyl-5-trifluoromethoxy-2-oxoindolin-3-yl acetate (3 g). Orange oil, yield: 88 %; ^{1}H NMR (400 MHz, $CDCl_3$): $\delta = 7.19$–7.08 (m, 2H), 6.80 (d, $J = 8.5$ Hz, 1H), 5.89–5.75 (m, 1H), 5.64–5.49 (m, 1H), 5.36–5.23 (m, 2H), 5.14–5.03 (m, 2H), 4.38–4.29 (m, 2H), 2.83 (m, 1H), 2.56 (dd, $J = 13.4$, 8.3 Hz, 1H), 2.08 (s, 3H); ^{13}C APT NMR (101 MHz, $CDCl_3$): $\delta = 173.88$, 168.94, 141.50, 130.77, 128.78, 128.41, 122.42, 121.19, 117.98, 116.99, 111.98, 109.82, 92.26, 78.98, 42.64, 40.80, 20.51; ^{19}F NMR (376 MHz, $CDCl_3$): $\delta = -58.42$ (s); HRESIMS: calcd for $(M + Na)^+$, 378.0929; found, 378,0917.

1,3-Diallyl-4,7-dichloro-2-oxoindolin-3-yl acetate (3 h). Orange oil, yield: 70 %; ^{1}H NMR (400 MHz, $CDCl_3$): $\delta = 7.03$ (d, $J = 8.8$ Hz, 1H), 6.78 (d, $J = 8.8$ Hz, 1H), 5.76 (ddd, $J = 12.6$, 10.5, 5.2 Hz, 1H), 5.19–5.12 (m, 2H), 5.01 (dt, $J = 10.6$, 1.5 Hz, 1H), 4.92 (t, $J = 1.5$ Hz, 1H), 4.89–4.83 (m, 2H), 4.52 (dq, $J = 5.2$, 1.7 Hz, 2H), 3.00 (q, $J = 7.1$ Hz, 2H), 2.51 (s, 3H)·^{13}C APT NMR (101 MHz, $CDCl_3$): $\delta = 166.38$, 162.88, 132.96, 132.57, 128.43, 128.12, 124.25, 121.05, 116.53, 43.44, 37.92, 36.38, 31.22, 21.82, 20.39, 19.70.; HRESIMS: calcd for $(M + Na)^+$, 362.0327; found, 362.0318.

1,3-Diallyl-7-trifluoromethyl-2-oxoindolin-3-yl acetate (3i). Yellow oil, yield: 88 %; ^{1}H NMR (400 MHz, $CDCl_3$): $\delta = 7.63$–7.34 (m, 2H), 7.10 (t, $J = 8.2$ Hz, 1H), 5.93–5.71 (m, 1H), 5.59–5.43 (m, 1H), 5.25–4.97 (m, 4H), 4.57–4.45 (m, 2H), 2.78 (m, 1H), 2.59 (m, 1H), 2.08 (s, 3H); ^{13}C APT NMR (101 MHz, $CDCl_3$): $\delta = 175.22$, 168.78, 140.94, 131.51, 130.29, 128.65, 127.51, 126.23, 124.72, 122.01, 121.87, 121.25, 116.77, 77.35, 44.62, 41.21, 20.46; ^{19}F NMR (376 MHz, $CDCl_3$): $\delta = -55.04$ (s); HRESIMS: calcd for $(M + Na)^+$, 362.0980; found, 362.0969.

2.4. General procedure for the synthesis of compounds 6a-6c

Compounds **4a-4c** were prepared based on the procedure used for **1a-1i** but using benzyl bromide (7.80 mmol) as reagent. Compounds **5a-5c** were prepared following the procedure used for **2a-2i**. Compounds **6a-6c** were prepared following the procedure used for **3a-3i**.

1-Benzyl-5-nitroindolin-2,3-dione (4a). Orange powder, yield: 80 %, m.p: 167.8 °C (literature: 166–167 °C)[23]; ^{1}H NMR (400 MHz, $CDCl_3$): $\delta = 8.48$ (d, $J = 2.3$ Hz, 1H), 8.42 (dd, $J = 8.7$, 2.4 Hz, 1H), 7.42–7.31 (m, 5H), 6.93 (d, $J = 8.7$ Hz, 1H), 5.02 (s, 2H); ^{13}C APT NMR (101 MHz, $CDCl_3$): $\delta = 158.04$, 154.85, 133.64, 133.48, 129.53, 128.88, 127.59, 121.17, 111.38, 44.75; HRESIMS: calcd for $(M + Na)^+$, 305.0538; found, 305.0528.

1-Benzyl-5-methoxyindolin-2,3-dione (4b). Red-brown powder, yield: 99 %, m.p: 95.3 °C; ^{1}H NMR (400 MHz, $CDCl_3$): $\delta = 7.38–7.27$ (m, 5H), 7.15 (d, $J = 2.7$ Hz, 1H), 7.02 (dd, $J = 8.6$, 2.7 Hz, 1H), 6.67 (d, $J = 8.6$ Hz, 1H), 4.90 (s, 2H), 3.77 (s, 3H); ^{13}C APT NMR (101 MHz, $CDCl_3$): $\delta = 158.52$, 156.69, 144.76, 134.72, 129.18, 128.28, 127.55, 124.85, 118.25, 112.17, 109.68, 56.09, 44.21, 29.84.; HRESIMS: calcd for $(M + H)^+$, 268.0974; found, 268.0965.

1-Benzyl-4,7-dichloroindolin-2,3-dione (4c). Orange powder, yield: 96 %, m.p: 209.0 °C; ^{1}H NMR (400 MHz, $CDCl_3$): δ =7.40–7.24 (m, 6H), 7.02 (d, $J = 8.7$ Hz, 1H), 5.39 (s, 2H). ^{13}C APT NMR (101 MHz, $CDCl_3$): $\delta = 140.79$, 135.93, 133.22, 129.01, 127.97, 126.68, 115.83, 45.30.; HRESIMS: calcd for $(M + Na)^+$, 327.9908; found, 327.9898.

3-Allyl-1-benzyl-3-hydroxy-5-nitroindolin-2-one (5a). Orange oil, yield: 98 %; ^{1}H NMR (400 MHz, $CDCl_3$): $\delta = 8.11–7.93$ (m, 3H), 7.12 (d, $J = 3.5$ Hz, 5H), 6.64 (d, $J = 8.7$ Hz, 1H), 5.44–5.28 (m, 1H), 4.93–4.80 (m, 4H), 4.67 (d, $J = 15.7$ Hz, 2H), 2.65–2.52 (m, 2H).;^{13}C APT NMR (101 MHz, $CDCl_3$) $\delta = 177.80$, 162.69, 147.90, 143.17, 134.41, 131.50, 129.85, 128.57, 127.65, 127.02, 125.93, 120.35, 119.62, 108.70, 75.22, 43.65, 42.22, 36.43, 35.33, 31.26; Mass (ESI+) $m/z = 325.27$ $(M + H)^+$.

3-Allyl-1-benzyl-3-hydroxy-5-methoxyindolin-2-one (5b). Orange oil, yield: 99 %; ^{1}H NMR (400 MHz, $CDCl_3$): $\delta = 7.34–7.26$ (m, 5H), 7.01 (d, $J = 2.6$ Hz, 1H), 6.75–6.69 (m, 1H), 6.59 (d, $J = 8.5$ Hz, 1H), 5.65 (dddd, $J = 16.6$, 10.1, 8.5, 6.2 Hz, 1H), 5.21–5.10 (m, 2H), 4.99 (d, $J = 15.7$ Hz, 1H), 4.71 (d, $J = 15.7$ Hz, 1H), 3.76 (s, 3H), 2.89 (s, 1H), 2.82–2.64 (m, 2H); ^{13}C APT NMR (101 MHz, $CDCl_3$): $\delta = 177.75$, 156.46, 135.62, 130.99, 130.62, 128.89, 127.80, 127.42, 120.77, 114.32, 111.39, 110.16, 76.39, 55.95, 44.06, 43.29, 32.07, 29.84, 29.50, 22.83, 14.25.Mass (ESI+) $m/z = 310.24$ $(M + H)^+$.

3-Allyl-1-benzyl-3-hydroxy-4,7-dichloroindolin-2-one (5c). Yellow powder, yield: 86 %, m.p:155.5 °C - 156 °C; ^{1}H NMR (400 MHz, $CDCl_3$): $\delta = 7.32–7.19$ (m, 5H), 7.13 (d, $J = 8.8$ Hz, 1H), 6.97 (d, $J = 8.7$ Hz, 1H), 5.40 (dddd, $J = 16.9$, 10.0, 8.2, 6.7 Hz, 1H), 5.30 (s, 2H), 5.14 (dq, $J = 17.0$, 1.3 Hz, 1H), 5.05–5.01 (m, 1H), 3.22 (ddt, $J = 12.9$, 6.8, 1.2 Hz, 1H), 3.01 (s, 1H), 2.96–2.88 (m, 1H); ^{13}C APT NMR (101 MHz, $CDCl_3$): $\delta = 177.13$, 140.23, 136.54, 133.03, 130.13, 129.39, 128.40, 128.06, 127.16, 126.26, 124.92, 120.91, 114.26, 44.80, 40.10, 31.75, 31.26, 30.01, 29.53, 29.19, 22.52, 13.95.; Mass (ESI+) m/z = 350.19 $(M + H)^+$.

3-Allyl-1-benzyl-5-nitro-2-oxoindolin-3-yl acetate (6a). Yellow oil, yield: 84 %; ^{1}H NMR (400 MHz, $CDCl_3$): $\delta = 2.19$ (s, 3H), 2.98 (dddt, 2H), 4.85–5.11 (m, 4H), 5.50 (dq, $J = 8.2$, 16.5 Hz, 1H), 7.25–7.37 (m, 5H), 6.69 (dd, $J = 8.7$, 18.1 Hz, 1H), 8.01–8.17 (m, 2H); ^{13}C APT NMR (101 MHz, $CDCl_3$): $\delta = 21.7$, 40.6, 44.0, 78.3, 109.1, 118.6, 121.5, 126.4, 127.2, 127.2, 127.8, 128.0, 128.0, 128.4, 128.7, 134.4, 143.2, 148.2, 166.5, 175.7; Mass (ESI+) m/z = 389.08 $(M + Na)^+$.

3-Allyl-1-benzyl-5-methoxy-2-oxoindolin-3-yl acetate (6b). Red-brown oil, yield: 97 %; ^{1}H NMR (400 MHz, $CDCl_3$): $\delta = 7.36–7.28$ (m, 4H), 7.26–7.21 (m, 1H), 6.82 (d, $J = 2.6$ Hz, 1H), 6.67 (dd, $J = 8.6$, 2.6 Hz, 1H), 6.52 (d, $J = 8.5$ Hz, 1H), 5.56 (dddd, $J = 16.6$, 10.1, 8.3, 6.2 Hz, 1H), 5.14–5.05 (m, 2H), 4.90 (d, $J = 1.9$ Hz, 2H), 3.72 (s, 3H), 2.85 (ddt, $J = 13.4$, 6.2, 1.8 Hz, 1H), 2.64 (ddt, $J = 13.5$, 8.3, 0.9 Hz, 1H), 2.07 (s, 3H); ^{13}C APT NMR (101 MHz, $CDCl_3$): $\delta = 174.07$, 168.85, 155.83, 136.24, 135.67, 129.41, 128.68, 128.48, 127.48, 127.26, 120.83, 113.35, 110.61, 109.87, 79.66, 55.71, 44.12, 41.19, 29.71, 20.68; HRESIMS: calcd for $(M + Na)^+$, 374.1368; found, 374.1357.

3-Allyl-1-benzyl-4,7-dichloro-2-oxoindolin-3-yl acetate (6c). Yellow oil, yield: 89 %; ^{1}H NMR (400 MHz, $CDCl_3$): $\delta = 7.31$ (d, $J = 4.4$ Hz, 4H), 7.25–7.22 (m, 1H), 7.12 (d, $J = 8.8$ Hz, 1H), 6.91 (d, $J = 8.8$ Hz, 1H), 5.40–5.21 (m, 3H), 5.08 (dq, $J = 17.0$, 1.4 Hz, 1H), 5.01 (ddt, $J = 10.1$, 1.8, 0.9 Hz, 1H), 3.20 (ddt, $J = 13.1$, 7.1, 1.2 Hz, 1H), 2.90 (ddt, $J = 13.1$, 7.7, 1.0 Hz, 1H), 2.14 (s, 3H); ^{13}C APT NMR (101 MHz, $CDCl_3$): $\delta = 174.09$, 169.07, 140.72, 137.31, 133.12, 128.67, 128.47, 128.33, 127.12, 126.50, 126.11, 124.49, 121.44, 114.26, 79.42, 45.19, 38.30, 29.73, 20.11; HRESIMS: calcd for $(M + Na)^+$, 412.0483; found, 412.0474.

2.5. General procedure for the synthesis of compounds 8a-8c

Compounds **7a-7c** were prepared following a procedure described in the literature.[20]

Starting from the corresponding **1d**, **1f** and **1 h** compounds (1.29 mmol) in DMF (6 mL), indium (2.58 mmol), sodium iodide (5.17 mmol), and benzyl bromide (5.17 mmol) were added. The reaction mixtures were stirred at room temperature for 8 h, and hydrochloric acid (10 % aqueous solution) was added to end the reactions. After extraction with dichloromethane, the products were washed with brine and dried over anhydrous Na_2SO_4 to obtain the pure compounds **7a-7c**.

Compounds **8a-8c** were prepared following the procedure used for **3a-3i**.

1-Allyl-3-benzyl-3-hydroxy-5-nitroindolin-2-one (7a). Orange oil, yield: 79 %; ^{1}H NMR (400 MHz, $CDCl_3$): $\delta = 3.76–3.92$ (ddt, 2H), 4.16 (m, 2H), 4.85 (m, 2H), 5.28 (m, 1H), 6.70–7.55 (m, 6H), 7.70–7.78 (d, 2H); ^{13}C APT NMR (101 MHz, $CDCl_3$): $\delta = 42.1$, 44.3, 78.8, 110.0, 117.5120.0, 126.1, 127.8, 128.1, 129.2, 130.1, 131.4, 133.2, 133.5, 134.4, 141.6, 148.1, 177.5; Mass (ESI+) $m/z = 301.64$ $(M + Na)^+$.

1-Allyl-3-benzyl-3-hydrody-5-methoxyindolin-2-one (7b). Orange oil, yield: 80 %; ^{1}H NMR (400 MHz, $CDCl_3$): δ =7.12–7.06 (m, 3H), 6.95–6.91 (m, 3H), 6.74 (dd, $J = 8.5$, 2.6 Hz, 1H), 6.51 (d, $J = 8.5$ Hz, 1H), 5.41 (ddt, $J = 17.2$, 10.3, 5.1 Hz, 1H), 4.95 (dd, $J = 10.5$, 1.4 Hz, 1H), 4.70–4.65 (m, 1H), 4.32–4.26 (m, 1H), 3.91–3.85 (m, 1H), 3.75 (s, 3H), 3.37 (d, $J = 12.8$ Hz, 1H), 3.26 (d, $J = 12.8$ Hz, 1H); ^{13}C APT NMR (101 MHz, $CDCl_3$): $\delta = 177.84$, 156.15, 135.79, 134.03, 130.78, 130.76, 130.38, 127.85, 126.82, 117.21, 114.42, 111.19, 109.86, 78.13, 55.81, 45.01, 42.27, 29.72, 14.16; Mass (ESI+) m/z = 332.19 $(M + Na)^+$.

1-Allyl-3-benzyl-3-hydrody-4,7-dichloroindolin-2-one (7c). Yellow oil, yield: 78 %; ^{1}H NMR (400 MHz, $CDCl_3$): $\delta = 3.58–3.72$ (m, 2H), 5.02 (ddt, $J = 4.6$, 10.5, 17.3 Hz, 4H), 5.38 (m, 1H), 6.30–7.39 (m, 7H); ^{13}C APT NMR (101 MHz, $CDCl_3$): $\delta = 40.3$, 42.5, 79.0, 115.2, 122.3, 126.4, 126.8, 127.5, 127.7, 128.7, 129.2, 130.2, 132.2, 132.9, 134.0, 135.1, 142.7, 176.5; Mass (ESI+) m/z = 349.92 $(M + H)^+$.

1-Allyl-3-benzyl-5-nitro-2-oxoindolin-3-yl acetate (8a). Red-brown oil, yield: 97 %; ^{1}H NMR (400 MHz, $CDCl_3$): $\delta = 2.00$ (s, 3H), 2.91–3.40 (m, 2H), 4.25 (d, 2H), 5.03 (m, 2H), 5.55 (m, 1H), 7.11 (d, $J = 7.5$ Hz, 3H), 7.28–7.62 (m, 4H), 8.03–8.20 (m, 1H); ^{13}C APT NMR (101 MHz, $CDCl_3$): $\delta = 20.7$, 42.1, 44.5, 79.3, 108.8, 117.7, 119.9, 126.9, 127.9, 128.6, 129.1, 130.0, 130.5, 130.8, 133.1, 134.2, 143.2, 148.4, 166.3, 175.5; HRESIMS: calcd for $(M-H)^-$, 365.1143; found, 365.1146.

1-Allyl-3-benzyl-5-methoxy-2-oxoindolin-3-yl acetate (8b). Red oil, yield: 83 %; ^{1}H NMR (400 MHz, $CDCl_3$): $\delta = 2.03$ (s, $J = 1.3$ Hz, 3H), 3.02 (ddt, 2H), 3.69 (s, 3H), 4.62 (m, 2H), 5.04 (m, 2H), 6.32–6.57 (m, 1H), 6.99–7.14 (m, 4H), 7.44–7.52 (m, 3H), 7.82 (d, $J = 7.6$ Hz, 1H); ^{13}C APT NMR (101 MHz, $CDCl_3$): $\delta = 20.5$, 41.8, 44.9, 55.5, 79.1, 109.5, 111.2, 114.2, 117.1, 127.2, 128.1, 128.3, 129.1, 130.2, 130.8, 133.1, 134.2, 139.0, 156.2, 166.3, 175.3; HRESIMS: calcd for $(M-H)^-$, 350.1398; found, 350.1402.

1-Allyl-3-benzyl-4,7-dichloro-2-oxoindolin-3-yl acetate (8c). Yellow oil, yield: 93 %; ^{1}H NMR (400 MHz, $CDCl_3$): $\delta = 2.94$ (s, 3H), 3.77 (ddt, 2H), 4.39 (m, 2H), 4.60–4.71 (m, 2H), 5.50 (m, 1H), 6.83 (m, 1H), 7.35–7.56 (m, 5H), 7.75–7.88 (m, 1H); ^{13}C APT NMR (101 MHz, $CDCl_3$): $\delta = 21.9$, 41.2, 43.0, 80.5, 116.1, 124.6, 126.9, 127.7, 128.1, 128.3, 129.1, 129.6, 130.8, 131.9, 132.6, 133.1, 134.2, 140.2, 163.0, 175.0; HRESIMS: calcd for $(M + Na)^+$, 412.0483; found, 412.0472.

2.6. General procedure for the synthesis of compounds 11a-11c

Compounds **9a-9c** were prepared based on the procedure used for **1a-1i** but using 5-bromo-1-pentene (7.80 mmol) as reagent. Compounds **10a-10c** were prepared following the procedure used for **7a-7c.** Compounds **11a-11c** were prepared following the procedure used for **3a-3i**.

5-Nitro-1-(pent-4-en-1-yl)indolin-2,3-dione (9a). Orange oil, yield: 96 %; ^{1}H NMR (400 MHz, $CDCl_3$): $\delta = 8.53$ (dd, $J = 8.7$, 2.4 Hz,

1H), 8.47 (d, $J = 2.3$ Hz, 1H), 7.05 (d, $J = 8.7$ Hz, 1H), 5.80 (ddt, $J = 16.9$, 10.3, 6.6 Hz, 1H), 5.11–5.04 (m, 2H), 3.82 (dd, $J = 8.1$, 6.7 Hz, 2H), 2.21–2.14 (m, 2H), 1.84 (p, $J = 7.3$ Hz, 2H); ^{13}C APT NMR (101 MHz, $CDCl_3$): $\delta = 181.31$, 157.89, 155.06, 144.07, 136.40, 133.61, 121.11, 117.22, 116.39, 110.29, 40.32, 30.75, 26.16; Mass (ESI+) $m/z = 283.10$ $(M + Na)^+$.

5-Methoxy-1-(pent-4-en-1-yl)indolin-2,3-dione (9b). Red oil, yield: 74 %; ^{1}H NMR (400 MHz, $CDCl_3$): $\delta = 7.16$–7.10 (m, 2H), 6.83–6.78 (m, 1H), 5.80 (ddt, $J = 16.9$, 10.2, 6.6 Hz, 1H), 5.11–4.98 (m, 2H), 3.80 (s, 3H), 3.73–3.66 (m, 2H), 2.13 (ddd, $J = 8.1$, 6.6, 1.5 Hz, 2H), 1.83–1.74 (m, 2H); ^{13}C APT NMR (101 MHz, $CDCl_3$): $\delta = 28.0$, 30.8, 41.2, 55.7, 109.7, 112.3, 115.2, 120.2, 122.5, 137.2, 143.7, 158.1, 162.0, 181.7; Mass (ESI+) $m/z = 268.08$ $(M + Na)^+$.

4,7-Dichloro-1-(pent-4-en-1-yl)indolin-2,3-dione (9c). Brown oil, yield: 97 %; ^{1}H NMR (400 MHz, $CDCl_3$): $\delta = 7.43$ (d, $J = 8.7$ Hz, 1H), 7.01 (d, $J = 8.8$ Hz, 1H), 5.87–5.74 (m, 1H), 5.07 (dq, $J = 17.1$, 1.7 Hz, 1H), 5.01 (dq, $J = 10.2$, 1.4 Hz, 1H), 4.17–4.09 (m, 2H), 2.18–2.13 (m, 2H), 1.84 (dq, $J = 9.4$, 7.4 Hz, 2H); ^{13}C APT NMR (101 MHz, $CDCl_3$): $\delta = 157.67$, 147.31, 140.54, 136.92, 133.02, 126.25, 115.74, 115.26, 41.62, 41.19, 31.88, 30.74, 28.49; Mass (ESI+) $m/z = 284.11$ $(M + H)^+$.

3-Benzyl-3-hydroxy-5-nitro-1-(pent-4-en-1-yl)indolin-2-one (10a). Orange oil, yield: 94 %; ^{1}H NMR (400 MHz, $CDCl_3$): $\delta = 1.35$ (m, 2H), 1.81 (dd, $J = 7.3$ Hz, 2H), 3.57 (dt, $J = 7.6$, 14.8 Hz, 2H), 3.87–3.99 (m, 2H), 5.31 (m, 2H), 5.56–5.74 (m, 1H), 7.05–7.66 (m, 8H); ^{13}C APT NMR (101 MHz, $CDCl_3$): $\delta = 29.4$, 31.4, 36.3, 37.7, 79.0, 107.9, 115.0, 125.8, 126.8, 127.2, 128.2, 129.3, 130.0, 130.9, 133.2, 134.5, 138.9, 141.4, 148.6, 176.0; Mass (ESI+) m/z = 375.01 $(M + Na)^+$.

3-Benzyl-3-hydrody-5-methoxy-1-(pent-4-en-1-yl)indolin-2-one (10b). Red oil, yield: 95 %; ^{1}H NMR (400 MHz, $CDCl_3$): $\delta = 1.61$–1.76 (m, 2H), 1.94–2.27 (m, 2H), 3.55 (ddt, $J = 7.3$, 14.8 Hz, 2H), 3.66 (s, 3H), 4.16–4.26 (m, 2H), 4.79–4.85 (m, 2H), 5.51–5.68 (m, 1H), 6.96–7.79 (m, 8H); ^{13}C APT NMR (101 MHz, $CDCl_3$): $\delta = 29.5$, 31.4, 44.6, 48.5, 55.6, 79.7, 109.6, 111.2, 113.8, 114.9, 126.7, 128.1, 129.3, 130.2, 130.8, 133.2, 134.4, 137.6, 138.3, 155.5, 177.7; Mass (ESI+) m/z = 360.23 $(M + Na)^+$.

3-Benzyl-3-hydrody-4,7-dichloro-1-(pent-4-en-1-yl)indolin-2-one (10c). Yellow oil, yield: 91 %; ^{1}H NMR (400 MHz, $CDCl_3$): $\delta = 1.75$ (m, 2H), 2.38–2.55 (m, 2H), 3.15 (m, 2H), 3.50–3.67 (m, 2H), 4.71–4.93 (m, 2H), 5.52 (m, 1H), 6.63–7.73 (m, 7H); ^{13}C APT NMR (101 MHz, $CDCl_3$): $\delta = 27.7$, 31.4, 41.0, 44.4, 79.4, 114.8, 122.6, 126.6, 127.2, 128.0, 128.4, 128.9, 129.2, 130.7, 133.2, 134.3, 135.1, 137.3, 141.7, 177.4; Mass (ESI+) m/z = 398.98 $(M + Na)^+$.

3-Benzyl-5-nitro-2-oxo-1-(pent-4-en-1-yl)indolin-3-yl acetate (11a). Orange oil, yield: 80 %; ^{1}H NMR (400 MHz, $CDCl_3$): $\delta = 1.21$–1.49 (m, 2H), 2.39–2.43 (m, 2H), 2.45 (s, 3H), 3.41 (ddt, 2H), 3.81–3.96 (m, 2H), 4.81–4.91 (dd, 2H), 5.52–5.78 (m, 1H), 6.98–7.57 (m, 8H); ^{13}C APT NMR (101 MHz, $CDCl_3$): $\delta = 20.7$, 29.5, 31.4, 39.7, 42.0, 82.1, 110.7, 115.3, 120.0, 125.8, 127.0, 128.0, 128.4, 128.9, 129.5, 130.7, 134.4, 137.0, 141.6, 148.1, 170.6, 176.2; HRESIMS: calcd for $C_{17}H_{13}N_2O_5$ (fragment peak) 325.0824; found, 325.0835.

3-Benzyl-5-methoxy-2-oxo-1-(pent-4-en-1-yl)indolin-3-yl acetate (11b). Orange oil, yield: 75 %; ^{1}H NMR (400 MHz, $CDCl_3$): $\delta = 1.31$–1.50 (m, 2H), 2.55 (dd, $J = 8.4$, 13.5 Hz, 2H), 2.64 (s, 3H), 3.23–3.49 (m, 2H), 3.65 (s, 3H), 4.16 (m, 2H), 4.82–4.99 (m, 2H), 5.58–5.82 (m, 1H), 6.95–7.66 (m, 8H); ^{13}C APT NMR (101 MHz, $CDCl_3$): $\delta = 21.2$, 27.6, 30.6, 40.1, 42.4, 55.6, 82.2, 108.8, 110.5, 114.0, 115.0, 127.0, 128.1, 128.4, 128.9, 129.3, 129.6, 134.4, 137.5, 138.5, 155.5, 170.8, 176.6; HRESIMS: calcd for $(M + Na)^+$, 402.1681; found, 402.1671.

3-Benzyl-4,7-dichloro-2-oxo-1-(pent-4-en-1-yl)indolin-3-yl acetate (11c). Yellow oil, yield: 95 %; ^{1}H NMR (400 MHz, $CDCl_3$): $\delta = 1.83$ (m, 2H), 2.05 (m, 2H), 2.17 (s, 3H), 3.56–3.74 (m, 2H), 3.75–3.89 (m, 2H), 4.73–4.85 (m, 2H), 5.48–5.74 (m, 1H), 6.64–7.54 (m, 7H); ^{13}C APT NMR (101 MHz, $CDCl_3$): $\delta = 20.9$, 27.5, 31.5, 40.8, 44.6, 80.6, 114.8, 121.1, 127.2, 128.0, 128.4, 128.9, 129.2, 129.6, 129.9, 130.7, 133.2, 134.4, 137.0, 141.6, 169.0, 176.1; HRESIMS: calcd for $C_{17}H_{12}Cl_2NO_3$ (fragment peak) 348.0194; found, 348.0204 (^{35}Cl) and 350.0173 (^{37}Cl).

2.7. General procedure for the synthesis of compounds 12a-12d

To the corresponding derivatives (0.67 mmol) in dichloromethane (5 mL), pentafluoropropionic anhydride (2.01 mmol) and potassium tert-butoxide (catalytic amount) were added. The reaction mixtures were stirred at 30 °C for 8–10 h. After extraction with water, the products were washed with sodium bicarbonate and dried over anhydrous Na_2SO_4 to obtain the pure compounds **12a-12e.**

3-Allyl-1-benzyl-4,7-dichloro-2-oxoindolin-3-yl 2,2,3,3,3-pentafluoropropanoate (12a). Orange powder, yield: 82 %, m.p: 148.3 °C–149.2 °C; ^{1}H NMR (400 MHz, $CDCl_3$): $\delta = 2.92$ (dd, $J = 12.9$, 8.1 Hz, 1H), 3.23 (ddt, $J = 12.9$, 6.7, 1.2 Hz, 1H), 5.02 (dd, $J = 10.1$, 1.8 Hz, 1H), 5.13 (dq, $J = 17.1$, 1.5 Hz, 1H), 5.40 (dddd, $J = 16.9$, 10.0, 8.2, 6.8 Hz, 1H), 6.97 (d, $J = 8.8$ Hz, 1H), 7.13 (d, $J = 8.7$ Hz, 1H), 7.18–7.32 (m, 5H); ^{13}C APT NMR (101 MHz, $CDCl_3$) $\delta = 14.25$, 22.83, 29.50, 29.80, 29.84, 32.07, 40.40, 45.15, 114.59, 121.16, 125.27, 126.60, 127.48, 128.47, 128.71, 129.73, 130.49, 133.32, 136.86, 140.54, 177.61; ^{19}F NMR (376 MHz, $CDCl_3$) $\delta = -120.65$, −82.48.

3-Allyl-1-benzyl-5-nitro-2-oxoindolin-3-yl 2,2,3,3,3-pentafluoropropanoate (12b). Pale yellow powder, yield: 87 %; ^{1}H NMR (400 MHz, $CDCl_3$) $\delta = 2.68$–2.75 (m, 1H), 2.85 (ddt, $J = 13.4$, 6.3, 1.3 Hz, 1H), 4.81 (d, $J = 15.8$ Hz, 1H), 5.04 (d, $J = 15.7$ Hz, 1H), 5.14–5.23 (m, 2H), 5.64 (dddd, $J = 16.7$, 10.1, 8.5, 6.3 Hz, 1H), 6.79 (d, $J = 8.7$ Hz, 1H), 7.25 (d, $J = 1.5$ Hz, 1H), 7.26–7.38 (m, 4H), 8.18 (dd, $J = 8.7$, 2.3 Hz, 1H), 8.28 (d, $J = 2.3$ Hz, 1H); ^{13}C APT NMR (101 MHz, $CDCl_3$) $\delta = 43.07$, 44.40, 75.56, 109.37, 120.31, 122.06, 126.82, 127.39, 128.39, 129.23, 129.40, 130.62, 134.40, 143.97, 148.20, 178.05; ^{19}F NMR (376 MHz, $CDCl_3$) $\delta = -122.10$, −82.95.

1,3-Diallyl-5-fluoro-2-oxoindolin-3-yl 2,2,3,3,3-pentafluoropropanoate (12c). Orange powder, yield: 78 %, m.p: 61.4 °C-62.2 °C; ^{1}H NMR (400 MHz, $CDCl_3$) $\delta = 2.63$ (dd, $J = 13.3$, 8.3 Hz, 1H), 2.75 (ddt, $J = 13.3$, 6.4, 1.3 Hz, 1H), 4.17 (ddt, $J = 16.4$, 5.4, 1.7 Hz, 1H), 4.40 (ddt, $J = 16.4$, 5.1, 1.8 Hz, 1H), 5.07–5.14 (m, 2H), 5.18–5.24 (m, 2H), 5.55–5.65 (m, 1H), 5.78 (ddt, $J = 17.4$, 10.3, 5.2 Hz, 1H), 6.74 (dd, $J = 8.6$, 4.1 Hz, 1H), 6.98 (td, $J = 8.8$, 2.7 Hz, 1H), 7.15 (dd, $J = 7.6$, 2.6 Hz, 1H); ^{19}F NMR (376 MHz, $CDCl_3$) $\delta = -122.22$, −83.18.

1,3-Diallyl-4,7-dichloro-2-oxoindolin-3-yl 2,2,3,3,3-pentafluoropropanoate (12d). Yellow viscous oil, yield: 71 %; ^{1}H NMR (400 MHz, $CDCl_3$) $\delta = 3.00$ (ddt, $J = 13.2$, 7.7, 1.0 Hz, 1H), 3.31 (ddt, $J = 13.1$, 7.1, 1.1 Hz, 1H), 4.71 (dq, $J = 5.5$, 1.8 Hz, 2H), 5.07 (ddt, $J = 10.0$, 1.7, 0.9 Hz, 1H), 5.13 (dq, $J = 17.0$, 1.3 Hz, 1H), 5.22 (dq, $J = 10.4$, 1.4 Hz, 1H), 5.25–5.34 (m, 2H), 5.91 (ddt, $J = 17.3$, 10.3, 5.0 Hz, 1H), 6.97 (d, $J = 8.8$ Hz, 1H), 7.24 (d, $J = 8.8$ Hz, 1H); ^{13}C APT NMR (101 MHz, $CDCl_3$) $\delta = 1.17$, 29.86, 37.74, 44.20, 117.66, 122.48, 124.98, 127.21, 132.26, 134.43; ^{19}F NMR (376 MHz, $CDCl_3$) $\delta = -120.73$, −82.54.

2.8. Enzyme assays for determination of BACE1 activity

The ability of the compounds to inhibit BACE1 activity was evaluated through an enzymatic assay using the β-Secretase (BACE1) Activity Detection Kit (CS0010, Sigma). The assay is based on a convenient fluorescence resonance energy transfer (FRET) method, which detects an increase in fluorescence signal upon cleavage of the substrate by BACE1.

Briefly, recombinant BACE1 was pre-incubated with different compounds for 15 min at 37 °C, followed by the addition of the substrate 7-methoxycoumarin-4-acetyl-[Asn670, Leu671]-Amyloid β-Protein Precursor/A4 770 Fragment 667–676-(2,4-dinitrophenyl) Lys-Arg-Arg amide trifluoroacetate salt. The assay was conducted for 2 h at 37 °C according to the manufacturer's protocol. Fluorescence at 320 nm (excitation) and 405 nm (emission) was measured using a black, clear-bottom 96-well plate on a SpectraMax iD3 plate reader. All independent assays were performed in triplicate.

2.9. Docking studies

The LY2886721 ligand co-crystallized in the 4x7i structure of BACE1 was obtained from the Protein Data Bank (https://www.rcsb.org/, PDB code: 4x7i). The 3D structure of BACE1 inhibitors was also obtained from the PDB, while the structures of the compounds to be tested were predicted using high-precision Glide XP [Schrödinger, 2020] and the OPLS3e force field. Calculations were performed with and without water molecules, following previously described protocols.[19,24–26]

For the ChE docking studies, protein X-ray crystal structures were obtained from the Protein Data Bank (6O4W and 4EY7 for AChE and 4AQD, 7Q1M and 4BDS for BuChE). All protein structures were determined at high resolution. The structures were inspected and had resolutions of 2.35 Å, 2.35 Å, 2.5 Å, 2.79 Å and 2.10 Å, respectively. Hydrogen atoms were added with Maestro software [Schrödinger, 2023]. Docking was then performed by extra precision Glide XP [Schrödinger, 2023] with extended sampling, and the OPLS3e forcefield. Water molecules, ions and ligands were treated in all enzymes (604 W, EY7, 4AQD, 7Q1M, 4BDS) prior to docking.[26b] The search space coordinates were AChE enzyme; 6O4W – Centre X: 89.341 Y: 84.453 Z: −5.628, and 4EY7 - Centre X: -15.834 Y: -43.535 Z: 25.391; and BuChE enzyme; 4AQD - Centre X: 7.0 Y: -10.639 Z: -12.236, 7Q1M - Centre X: 19.553 Y: 42.576 Z: 41.06, and 4BDS - Centre X: 131.866 Y: 112.975 Z: −44.529, Dimensions X: 20.000 Y: 20.000 Z: 20.000. The docking binding poses were visualized using Maestro [Schrödinger, LLC].

2.10. Cellular assays for cytotoxicity evaluation

2.10.1. Cell culture

The N2A-APPswe murine neuroblastoma cell line, which stably overexpresses human APP carrying the Swedish mutation KM670/671NL, was maintained in DMEM medium supplemented with 1 % (*v*/v) FBS, 0.4 mg/mL geneticin, 3.7 g/L sodium bicarbonate, 1 % (v/v) non-essential amino acids, and 1 mM sodium pyruvate, as previously described.[27–29] The cell line was cultured at 37 °C in humidified atmosphere with 5 % CO_2 and 95 % air. Cells were used until passage #37.

2.10.2. MTT reduction assay for cytotoxicity evaluation

The metabolic activity of N2A-APPswe cells, reflecting their viability, was assessed using the reduction assay of 3-(4,5-dimethylthiazol-2-yl)-2,5-diphenyltetrazolium bromide (MTT), as previously described.[28] Cells were plated at a density of 75,000 cells/cm^2 and, 24 h later, incubated at 37 °C with different concentrations (10, 20, 50, 100 and 150 μM) of compound **12a** (the most promising as a BACE1 inhibitor). After a 24 h incubation period, the cells were washed with Krebs saline solution (132 mM NaCl, 4 mM KCl, 1.2 mM Na_2HPO_4, 1.4 mM $MgCl_2$, 6 mM glucose, 10 mM HEPES, 1 mM $CaCl_2$, pH 7.4) and incubated with MTT (0.5 mg/mL in Krebs saline solution) for 30 min at 37 °C. Finally, acidic isopropanol was added to dissolve the formazan crystals formed after the reduction of the MTT salt. Absorbance was measured at 570 nm and 620 nm at 37 °C using a SpectraMax iD3 plate reader. MTT reduction was expressed as a percentage of the absorbance values obtained for control cells (cells treated with DMSO, the solvent used to dissolve the compounds). All independent assays were performed in triplicate.

2.11. Enzymatic assays for cholinesterase activity determination

2.11.1. Evaluation of the percentage of inhibition of eeAChE and eqBuChE

Solutions of the different compounds were prepared at concentrations of 1.250 and 0.625 mM (pre-well concentrations) by dilution from a 10 mM stock solution. In a 96-well plate, 20 μL of each inhibitor, 55 μL of Tris-HCl buffer (0.05 M, pH 8.0), 125 μL of 5,5'-Dithiobis(2-nitrobenzoic acid)(DTNB) (3 or 1.6 mM) and 25 μL of *ee*AChE (0.03 U/mL) or *eq*BuChE (0.03 U/mL) were added. The mixture was incubated for 15 min at 37 °C. Subsequently, 25 μL of acetylcholine iodide (ATCI) (1.5 mM) or butyrylcholine iodide (BTCI) (0.8 mM) was added to each well, and the plate was incubated again for 15 min at 37 °C. Finally, the plate was read at 412 nm at 25 °C. All assays were performed in triplicate. The human BuChE was kindly provided to us by Oksana Lockridge from the Eppley Institute, University of Nebraska Medical Center.

2.11.2. IC_{50} determination

Solutions of the different compounds were prepared at concentrations ranging from 0.39 to 200 μM (in-well concentrations) by successive dilutions from a stock solution of the compound. In a 96-well plate, 20 μL of different inhibitor concentrations, 55 μL of Tris-HCl buffer (0.05, pH 8.0), 125 μL of DTNB (0.8 mM), and 25 μL of *eq*BuChE (0.03 U/mL). The mixture was incubated for 15 min at 37 °C. Subsequently, 25 μL of BTCI (0.8 mM) was added to each well, and the plate was incubated again for 15 min at 37 °C. The plate was read at 412 nm at 25 °C. All assays were performed in triplicate.

2.12. Statistical analysis

In the enzymatic assays for determining BACE1 activity and in the cellular assays for assessing cytotoxicity, results are expressed as mean ± standard error of the mean (SEM) from the indicated number of independent experiments. Data were tested for Gaussian distribution using D'Agostino and Pearson normality tests and the Shapiro-Wilk test. Statistical comparisons were performed using the nonparametric Kruskal-Wallis test, followed by Dunn's post hoc test for multiple comparisons or by one-way analysis of variance (ANOVA) followed by Dunnett's. A p-value <0.05 was considered statistically significant. Statistical analysis was conducted using GraphPad Prism 9.0 software (GraphPad, Software Inc., San Diego, EUA).

In the enzymatic assays for determining cholinesterase activity, results are expressed as mean ± standard error of the mean (SEM) from independent experiments. Kinetic parameters were obtained through non-linear regression analysis using GraphPad Prism 9.0 software (GraphPad, Software Inc., San Diego, EUA), and the graph was generated using Microsoft Excel (Windows 10).

3. Results and discussion

3.1. Design concept and synthesis of oxindole derivatives

Part of our structure-based inhibitor design was based on our previous work with *N*-benzyl oxindoles which have been shown to be good binders with the hydrophobic residues present in BuChE (Fig. 2(a)).[15] The current rational was to substitute the N- and 3-phenyl groups with allyl and other unsaturated side-chains. This same rational holds-up for designing novel BACE-1 inhibitors as the active site contains aromatic units like; Trp76, Tyr71, and Phe108, as well as a hydrophobic Val69 unit. More importantly considering that BACE-1 is an aspartyl protease and based on the mechanism of action of this enzyme[30]; we considered the incorporation of an appropriate acyl l unit on the 3-hydroxy group with the potential for covalent.

binding with the key nucleophilic residues such as aspartic acid units this potentially leading to acetylation of this residue (Fig. 2 (b), the model shows an acetyloxy analogue). As regards BuChE, this is a serine esterase containing a catalytic triad that consists of serine and histidine residues,[31] this also can potentially be acylated by appropriate acyloxyoxindole inhibitors (Fig. 2 (c)).

The first group of compounds synthesized was a range of 1,3-diallyl-3-hydroxyindolin-2-one derivatives (**2a-2i**). To obtain these compounds, a synthetic methodology was followed that involved *N*-alkylations at the *N*-1 position of the respective starting compounds, and In-mediated *Barbier* allylations at the C-3 position of the corresponding intermediates.

Starting from the respective isatin derivatives, *N*-alkylations were performed using allyl bromide, yielding compounds **1a-1i** (68–96 %).

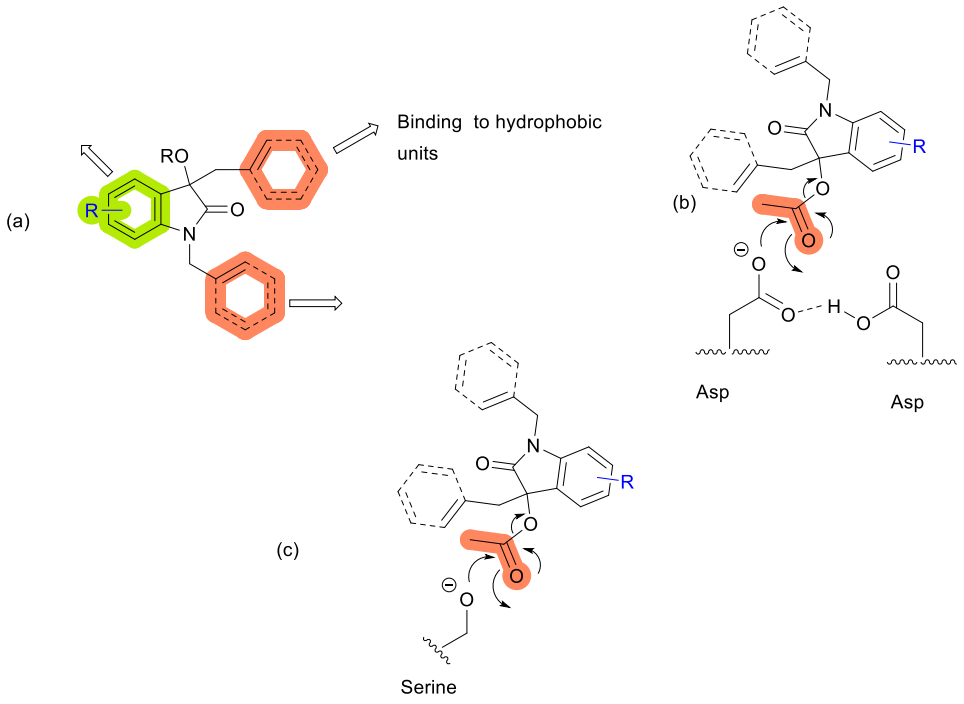

Fig. 2. Design concept. (a) Putative hydrophobic units present within BACE-1 and BuChE (see text) with novel unsaturated oxindoles (b) putative acetylation mechanism of BACE-1, and (c) putative acetylation mechanism of BuChE.

This was followed by In-mediated *Barbier* allylations with allyl bromide, resulting in compounds **2a-2i** (81–99 %) (Scheme 1). This reaction is superior to the Grignard reaction in certain cases like ours.

Next, a range of 1,3-diallyl-2-oxoindolin-3-yl acetate derivatives **3a-3i** was synthesized based on derivatives **2a-2i**, with an acetate group at the C-3 position instead of a hydroxyl group. The purpose of the modification was to assess its effect on binding efficiency to the active sites of BACE1 and cholinesterases. The rational was to establish covalent interactions with key nucleophilic residues in the active sites of both these proteins, by the presence of the acyloxy and olefinic units (see docking study). Besides olefins as pharmacophores are poorly studied despite their potential for forming key hydrophobic or π-π interactions with key active site residues. These compounds were obtained through alcohol acetylation reactions with acetic anhydride (52–88 %) (Scheme 2).

As shown in the following sections, the introduction of the acetate group had a significant effect on the binding affinity of the molecules to the active sites of the tested targets. For this reason, all subsequently synthesized molecules retained the acetate group, varying only the

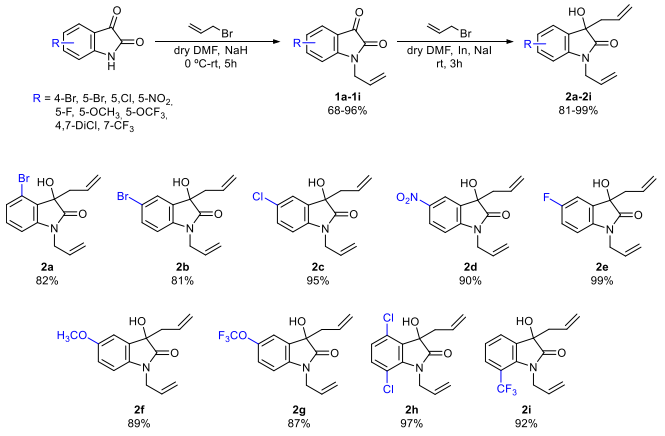

Scheme 1. Synthetic methodology to 1,3-diallyl-3-hydroxindolin-2-one derivatives (**2a-2i**).

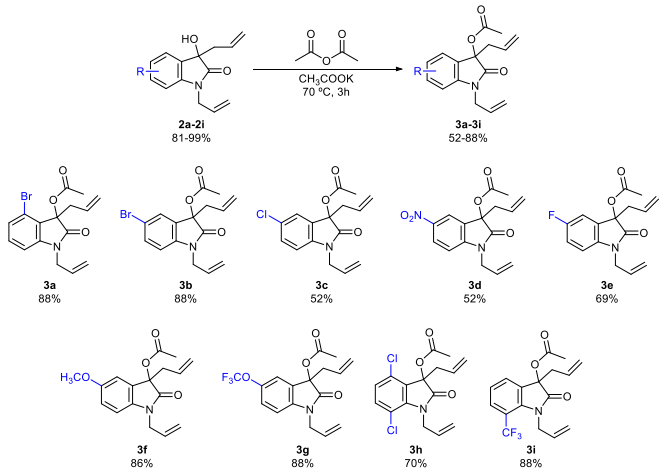

Scheme 2. Synthetic methodology to 1,3-diallyl-2-oxoindolin-3-yl acetate derivatives **3a-3i**.

substituents at *N*-1 and C-3 of the respective starting compounds, in an attempt to determine the effect of different substituents on the biological activity of the molecules relative to BACE1.

Thus, three types of compounds were synthesized: 3-allyl-1-benzyl-2-oxoindolin-3-yl acetate **6a-6c**, 1-allyl-3-benzyl-2-oxoindolin-3-yl acetate **8a-8c**, and 3-benzyl-2-oxo-1-(pent-4-en-1-yl)indolin-3-yl acetate **11a-11c**. For each type, three derivatives were synthesized with 5-nitro, 5-methoxy, and 4,7-dichloro substituents, as these had produced better results in BACE1 assays conducted on previous compounds.

Starting from 5-nitro-, 5-methoxy-, and 4,7-dichloroisatins, *N*-benzylations were performed using benzyl bromide, yielding compounds **4a-4c** (80–99 %). This was followed by In-mediated *Barbier* allylations with allyl bromide, resulting in compounds **5a-5c** (86–99 %). Finally, the compounds were acetylated with acetic anhydride, yielding derivatives **6a-6c** (84–97 %) (Scheme 3).

To obtain the 1-allyl-3-benzyl-2-oxoindolin-3-yl acetate derivatives

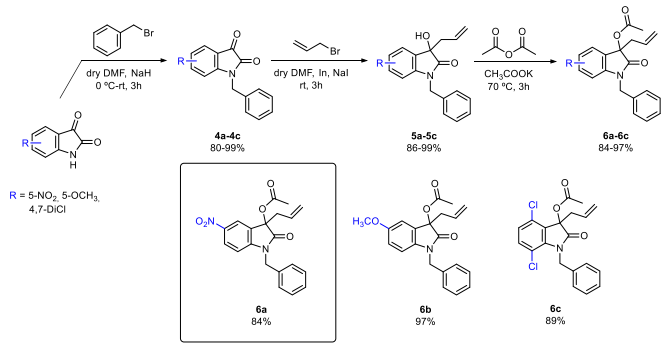

Scheme 3. Synthetic methodology to 3-allyl-1-benzyl-2-oxoindolin-3-yl acetate derivatives (**6a-6c**).

8a-8c, compounds **1d**, **1f** and **1 h** were used as starting materials followed by In-mediated *Barbier* reaction with benzyl bromide, yielding intermediates **7a-7c** (78–80 %). These compounds were then acetylated with acetic anhydride, resulting in the desired final compounds **8a** and **8b** (83–97 %) (Scheme 4). It was not possible to access compound **8c**.

The 3-benzyl-2-oxo-1-(pent-4-en-1-yl)indolin-3-yl acetate derivatives **11a-11c** were synthesized via *N*-alkylations with 5-bromo-1-pentene, yielding **9a-9c** (74–97 %), followed by In-mediated *Barbier* reactions with benzyl bromide, yielding **10a-10c** (91–95 %), and finally, acetylations with acetic anhydride, producing the final products **11a-11c** (75–95 %) (Scheme 5).

With the intention of improving the binding characteristics of our oxindole esters, a new family of fluorinated ester analogues was synthesized by acetylating intermediates **5a, 5c, 2e** and **2 h** with pentafluoropropionic anhydride, resulting in the desired products **12a**, **12b**, (Scheme 6) **12c** and **12d** (Scheme 7).

3.2. BACE1 inhibitory activity of oxindole derivatives

Almost all the synthesized compounds were evaluated, at a concentration of 10 μM, for their ability to inhibit BACE1. **12d** was not evaluated due to solubility issues. The results obtained in the assay are summarized in Table 1. In the same table, it is evident that several compounds exhibited values exceeding 100 %, which most likely occurred due to their inherent fluorescence. The compounds that showed the most promising results were (**3d**, **8a** and **12a**, the first two containing nitro groups) which were then selected for retesting, with a total of 3–5 independent experiments conducted. In parallel, we tested a reference inhibitor of BACE1 (β-Secretase Inhibitor IV - CAS 797035–11-1 - Calbiochem), at a concentration of 15 nM, as a positive control for the assay (data not shown). The results are depicted in Fig. 3.

Some of the compounds showed moderate inhibition of BACE-1 (Table 1). However, we became particularly interested in the fluorinated ester **12a**. **12a** is a moderate BACE1 inhibitor with a percentage of

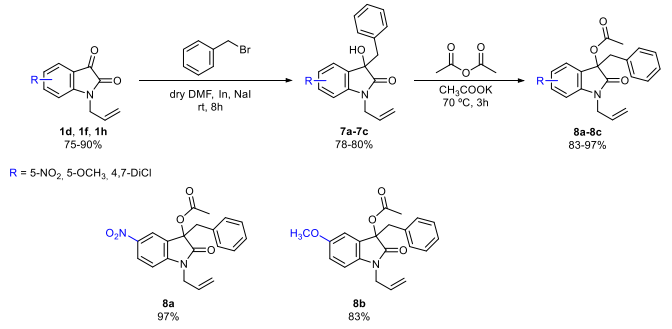

Scheme 4. Synthetic methodology to 1-allyl-3-benzyl-2-oxoindolin-3-yl acetate derivatives **8a-8c**.

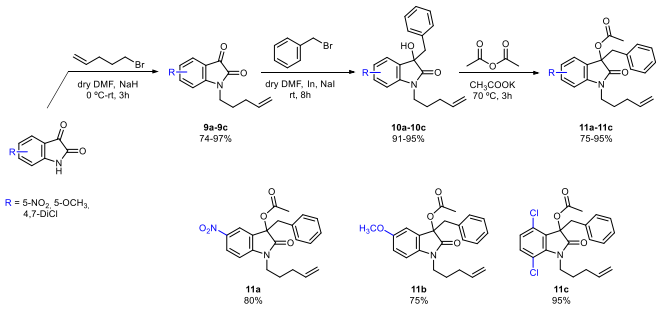

Scheme 5. Synthetic methodology to 3-benzyl-2-oxo-1-(pent-4-en-1-yl)indolin-3-yl acetate derivatives (**11a-11c**).

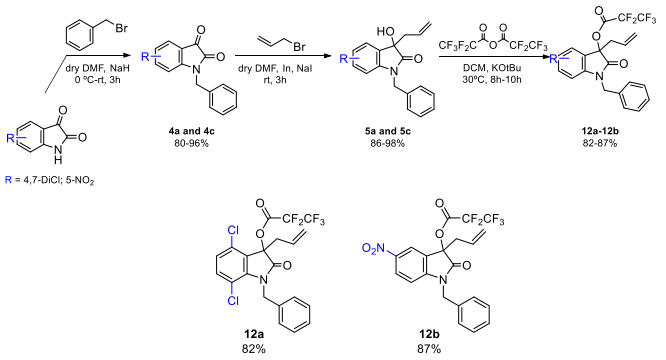

Scheme 6. Synthetic methodology of 3-allyl-1-benzyl-2-oxoindolin-3-yl 2,2,3,3,3-pentafluoropropanoate derivatives **12a-12b**

20.10 % (BACE1 activity of 79.90 %) (Figs. 3 and 4). Gratifyingly it was found to also inhibit both AChE, BuChE (including *h*BuChE), see Table 3 below. In the interest of developing further future analogues, consequently, it was subjected to docking studies to elucidate its binding pose in the enzyme's active site.

These results indicate that the presence of a nitro-group (**3d** and **8a**) in the 6-position appears to enhance the molecules binding capacity with the enzyme (see the inhibition values in Table 1 for these compounds).

Overall, it can be observed that the acetylated derivatives **3** gave reasonable results and this might be due to the design hypothesis proposed in Fig. 2 (b) above. Support for this hypothesis comes from the molecular docking study detailed in *sec*. 3.3, where close proximity of the Asp residue to the ligand is evident. However, it should be noted that BACE-1 can also catalyse the deprotonation of water molecules to form hydroxide that can hydrolyse the acetylated inhibitor,[30] thus potentially reducing the inhibitory effect of these ligands (i.e. prohibiting the acetylation of the enzyme itself). Assuming that our design model is relevant, this might explain why the inhibition is lower than that of the reference inhibitor LY2886721 (Table 2).

3.3. Docking study of 12a and 3 h

To gain an insight into the mode of action of our inhibitors we performed a docking study with compound **12a**. These studies were carried out on both enantiomers of **12a** (Figs. 5 and 6).

The docking scores (are generally imprecise, but do give an indication of the ligand-enzyme fit) for the two enantiomers were very good, the (*S*)-enantiomer with a better docking score than the (*R*)-enantiomer, and both showing better docking scores than AZD3293 a recognized and clinically evaluated BACE-1 inhibitor (Table 2). However, this calculation does not correlate with the bioassay studies, which is difficult to explain at this juncture, but could be a consequence of ester hydrolysis as discussed above (or the use of individual enantiomers for the docking

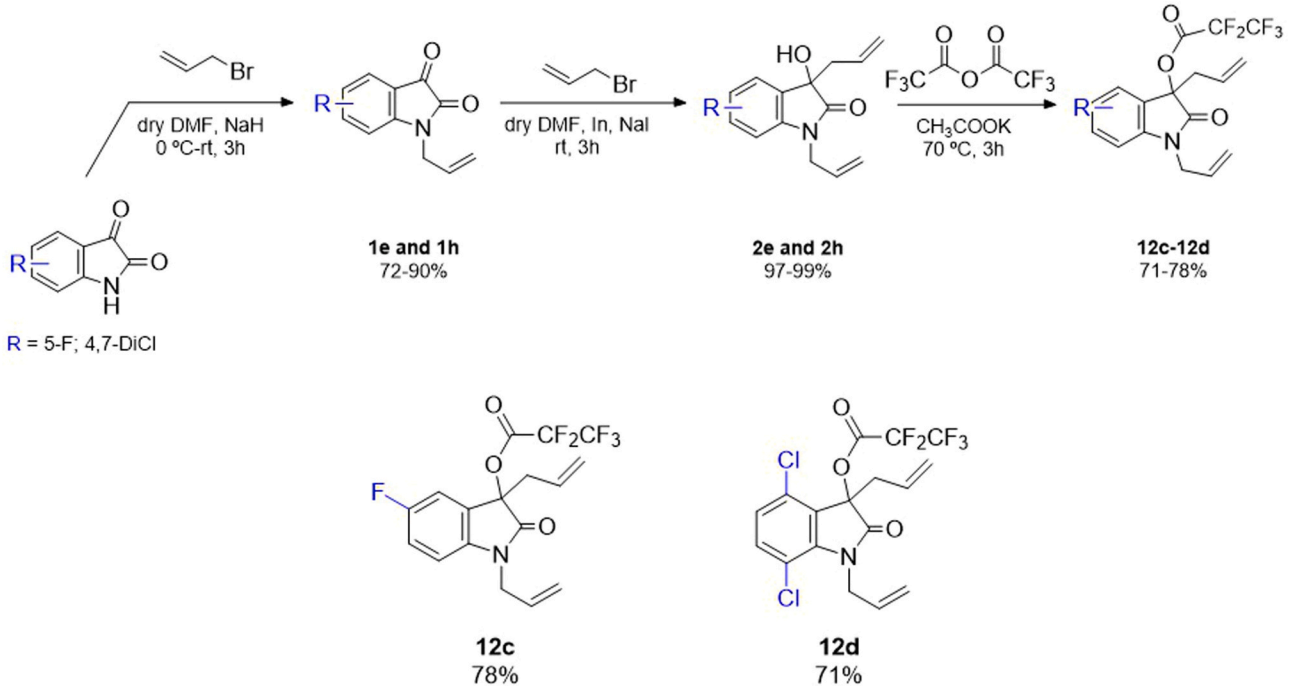

Scheme 7. Synthetic methodology to 1,3-diallyl-4,7-dichloro-2-oxoindolin-3-yl 2,2,3,3,3-pentafluoropropanoate derivatives **12c-12d.**

Table 1
Percentage of BACE1 activity in the presence of the 27 inhibitors tested.

Inhibitor	% BACE1 Activity	Inhibitor	% BACE1 Activity	Inhibitor	% BACE1 Activity
2a	>100	**3b**	83.04	**6c**	91.35
2b	>100	**3c**	82.09	**8a**	62.05
2c	>100	**3d**	65.72	**8b**	>100
2d	>100	**3e**	73.65	**11a**	91.38
2e	>100	**3f**	>100	**11b**	>100
2f	>100	**3 g**	>100	**11c**	>100
2 g	>100	**3 h**	>100	**12a**	79.90
2 h	>100	**3i**	90.76	**12b**	>100
2i	>100	**6a**	93.31	**12c**	>100
3a	85.68	**6b**	>100		
Reference	45.05 (average value, $n = 4$)				

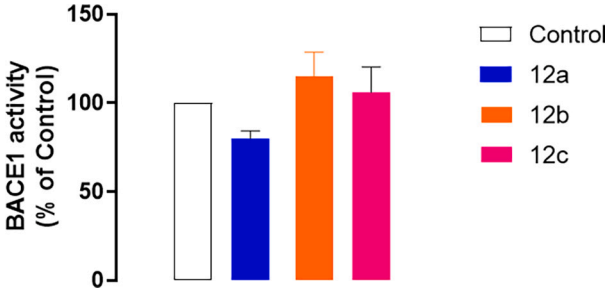

Fig. 3. Effect of the three inhibitors (**12a**, **12b** and **12c**) on BACE1 activity. The enzyme was pre-incubated with 10 μM of the respective inhibitors for 15 min, followed by substrate addition and incubation for 2 h. The reaction control corresponds to the enzymatic assay performed in the absence of inhibitors, including an equivalent concentration of DMSO, the solvent used to dissolve the compounds. The results, expressed as a percentage of the control, represent the mean ± SEM of 3–5 independent experiments in triplicate.

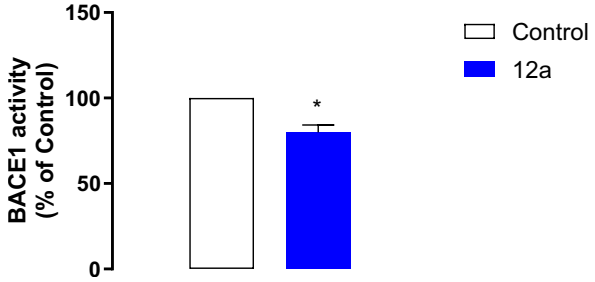

Fig. 4. Effect of the **12a** inhibitor on BACE1 activity. * $p < 0.05$: significantly different compared to the CTRL.

studies as opposed to the racemic mixture for the bioassay).

In the case of (*S*)-**12a** the ester group of the inhibitor is positioned relatively closely to the two serine units and the inhibitor may function via serine acylation (Fig. 2 (c)). The aspartate groups (32 and 228) are positioned farther away from this unit, with Asp32 being the closer unit. In the case of (*R*)-**12a** the serine units are more distant, but the Asp228 and Asp32 are relatively close.

The reference ligand used was LY2886721 (Fig. 6), co-crystallized in the 4x7i structure of BACE1. The remaining compounds are known BACE1 inhibitors. (*S*)- and (*R*)-**3 h** correspond to the enantiomers of the **3 h** inhibitor (used as comparison with **12a**) and (*S*)- and (*R*)-**12a** correspond to the enantiomers of the **12a** inhibitor. Ligand efficiency is calculated as the ratio between the docking score and the molecular weight of the inhibitors.

Surprisingly the calculated docking scores for both enantiomers of **12a** and (*S*)-**3 h** were better than that for the recognized BACE1 inhibitor drug **AZD3293**[5,32] which is a better inhibitor than the *rac*-**12a** and *rac*-**3 h** (bioassay of the racemates may be an explanation for this). Furthermore, the results revealed that the (*S*)-enantiomer in either case is the eutomer (with the highest inhibitory activity), suggesting that a potential separation and individual evaluation of the enantiomers might be worthwhile in the future (Table 2).

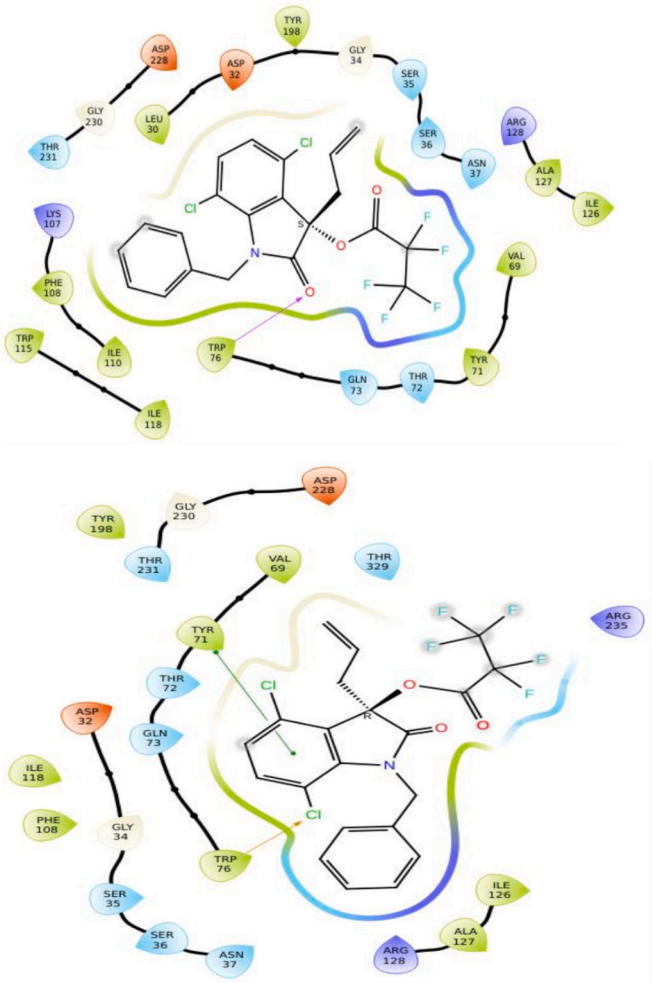

Fig. 5. Cross-Dock diagram. Binding of (*R*)-**12a** and (*S*)-**12a** into BACE1.

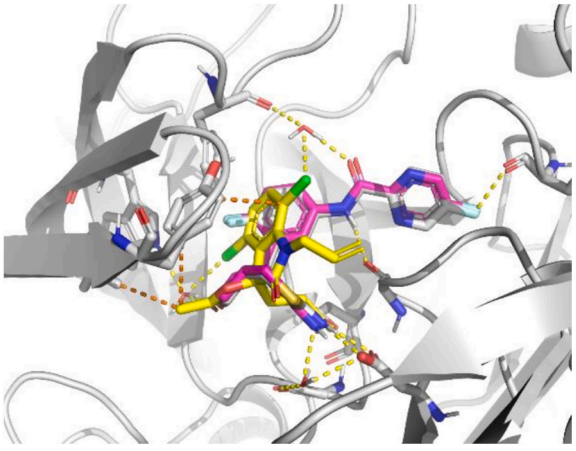

Fig. 6. Binding of (*S*)-**3 h** to the active site of BACE1. The co-crystallized ligand **LY2886721** is shown in magenta in the 4x7i structure of BACE1 (white), and the inhibitor (*S*)-**3 h** is shown in yellow. The residues in contact with the inhibitor are Ser10, Asp32, Gly34, Val69, Tyr71, Trp76, Phe108, Gly230 e Asp228, and the water molecules are HOH726, HOH930 e HOH900. Hydrogen bonds are represented by yellow dashed lines (– – -) and aliphatic or aromatic contacts are represented by orange dashed lines (– – -).

Table 2
Docking study against BACE-1.

Inhibitor	Docking score (kcal/mol)	Ligand efficiency
LY2886721	−11.6	−0.43
(*S*)-12a	−9.64	−0.30
(*R*)-12a	−8.81	−0,275
(*S*)-3 h	−6.40	−0.29
AZD3293	−6.06	−0.19
(*R*)-3 h	−4.26	−0.19

As a comparison we also conducted a docking study with the (*S*)-**3 h** inhibitor, which was the more potent enantiopode (Table 2) and indeed has the ability to bind to the enzyme's active site, establishing various interactions with the amino acid residues present including Asp228 and the serine residues (Fig. 6). However, it is difficult to explain the low potency from bioassay studies of this compound, which maybe was a consequence of acetate hydrolysis during the assay.

3.4. Evaluation of the 12a derivative cytotoxicity

A possible cytotoxic effect of inhibitor **12a** was evaluated in a murine neuroblastoma cell line overexpressing APPswe (N2A-APPswe cells) using a 3-(4,5-dimethylthiazol-2-yl)-2,5-diphenyltetrazolium bromide (MTT) reduction assay.[33] The results are presented in Fig. 7 and suggest that inhibitor **12a** does not induce toxicity in N2A-APPswe cells at concentrations of up to 100 μM. At 150 μM there is a reduction of approximately 24 % (Fig. 7).

3.5. AChE and BuChE inhibitory activity of 2a-2i and 3a-3i derivatives

In an attempt to find novel, multi-target-directed ligands (MTDLs) in another study, several of our synthesized compounds were selected for ChE bioassays in relavant models that included; eel AChE (*electrophorus electrius*, *ee*AChE), equine serum BuChE (*eq*BuChE) and human BuChe, using galantamine as a positive control. As discussed above, in the past our hydroxy-oxindole compounds have been shown to be good BuChE inhibitors, and family **3** and **12** were of special interest due to the presence of the ester units which can potentially bind to the cholinesterase (Fig. 2 (c)) as is the case of the substrate acetylcholine and the known inhibitor rivastigmine (containing a labile carbamate unit). The results obtained regarding ChE activity are reported in Table 3.

In general, these compounds were weak inhibitors of AChE (results consistent with those obtained for other analogous compounds developed by our group). However, more promising results were observed for BuChE inhibition, and compounds **2b**, **3a**, **3b**, **3d** and **12a** gave some moderate inhibition values. Again, it was mostly the ester analogues, and begs the question of the operation of an inhibition mechanism akin

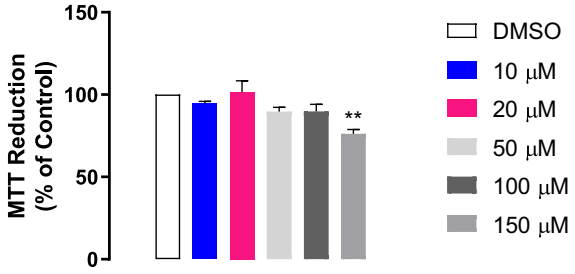

Fig. 7. Effect of inhibitor **12a** on cell viability. N2A-APPswe cells were incubated with different concentrations of inhibitor **12a** (10–150 μM) in culture medium containing 10 % FBS for 24 h. Cells treated with DMSO were used as controls, and their absorbance values were set as 100 %. The results, expressed as a percentage of the control, represent the mean ± SEM of three independent experiments performed in triplicate. ** $p < 0.01$: significantly different compared to the CTRL.

Table 3
Effect of inhibitors on *ee*AChE, *eq*BuChE and *h*BuChE activity and IC_{50} results for the best-performing compounds.

Inhibitor	*ee*AChE		eqBuChE		
	Inhibition %		Inhibition %		$IC_{50} \pm SD$ (μM)
	50 μM	100 μM	50 μM	100 μM	
2a	21	21	6	18	>100
2b	20	32	56	92	**35.5 ± 2.2**
2c	16	20	24	19	>100
2d	23	44	16	19	>100
2e	20	20	16	20	>100
2f	18	45	24	19	>100
2g	19	31	18	12	>100
2h	17	15	–	22	>100
2i	21	22	28	21	>100
3a	6	14	43	80	**60.3 ± 6.4**
3b	28	17	61	98	**23.8 ± 1.8**
3c	21	19	20	23	>100
3d	6	8	47	68	**45.9 ± 4.3**
3e	9	11	25	42	>100
3f	1	4	27	26	>100
3g	10	12	44	54	>100
3h	12	16	32	41	>100
3i	17	24	27	37	>100
12a	44	77	65	88	**68.5 ± 5.4** (*ee*AChE) **44.0 ± 6.0** **35.9 ± 2.7** (*h*BuChE)
12b	4	11	3	15	>100
12c	4	24	7	27	>100
Galantamine	89	100	77	100	37

In the enzyme activity measurements, *ee*AChE, *eq*BuChE and *h*BuChE were incubated with the compounds at concentrations of 50 and 100 μM for 15 min, followed by the addition of acetylcholine iodide (ATCI) and butyrylcholine iodide (BTCI), respectively, and further incubation for 15 min. Galantamine was used as a control. The experiments were performed in triplicate.
The dose-response curves are shown in the SI (Fig. s48 and s49).

to that outlined in Fig. 2(b). The best result to date was obtained using 1,3-diallyl-5-bromo-2-oxoindolin-3-yl acetate **3b**, which showed an IC_{50} value of 23.8 μM. This might also be due to the 6-Br unit, leading to key non-covalent interactions between this atom and some active site residues. In fact, the 6-bromo unit is also present in **2b** which is also one of the best inhibitors. In the case of **3d** the nitro group in the same position might be responsible for binding to the active site, thus substantiating this point-of-view that an electron-withdrawing group in the 6-position is required for binding in the active site. Moreover, it seems from these SAR studies, that a Br in this region (position-6 or 7) is good for binding as indicated by the inhibition observed for **3a**.

Given the good result for **12a** against *eq*BuChE it was screened against *h*BuChE and gratifyingly was found to be more potent against this target than the former (Table 3).

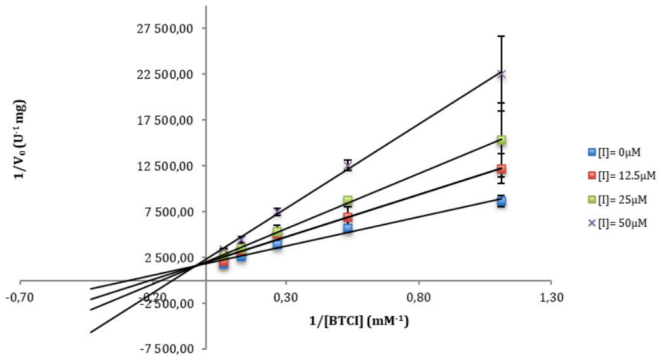

Fig. 8. Kinetic study of the inhibition mechanism of *eq*BuChE by compound **3b**. Lineweaver-Burk plot representing $1/V_0$ of *eq*BuChE versus 1/[BTCI] in the absence and presence of inhibitors.

The inhibition mechanism of *eq*BuChE was also studied using compound **3b** (Fig. 8). For this purpose, the Lineweaver-Burk was employed, providing a robust approach to determine kinetic parameters and identify the type of inhibition exerted by the compound, essential for understanding enzyme regulation in physiological contexts.

The reaction velocity (V_0) was studied in the absence and presence of their inhibitor (at concentrations of 12.5, 25 and 50 μM) across varying butyrylthiocholine iodide (BTCI) substrate concentrations (0.00, 0.90, 1.88, 3.75, 7.50 and 15.00 mM). The resulting graph, shown in Fig. 8, indicates mixed-type inhibition, with an inhibition constant (K_i) of 25.9 μM, which is considered moderate. This analysis indicated a decrease in V_{max} and an increase in K_M, reflecting mixed-type inhibition.

The intersection of the lines in the plot outside both the X and Y axes indicates a decrease in V_{max} in the presence of the inhibitor and an increase in K_M, reflecting mixed-type inhibition. This observation suggests that the inhibitor can bind both to the free enzyme (E) and the enzyme-substrate complex (ES), affecting both the V_{max} of the reaction and the enzyme's affinity for the substrate. In this case, inhibitor **3b** appears to interact with both the catalytic active site (CAS) and the peripheral anionic site (PAS), representing an intriguing result in terms of the *eq*BuChE inhibition efficacy.[11]

In the context of dual inhibition, compounds **3a**, **3b, 3d** and **12a** were the best examples (see Tables 1 and 3) from the screened library.

3.6. Docking Study against hAChE and hBuChE

To gain further insight into the nature of the interactions with the target docking studies were carried out. The results are shown in Table 4.

Table 4 shows the predicted and estimated docking scores for a cross-section of ligands (these values are quite imprecise). The results for (*R*)-**12a**, seem to imply that it is a strong binder for BuChE whereas the (*S*)-enantiopode is more selective for AChE. Unfortunately, these docking scores don't correlate very well with the measured inhibitions, as both **2a** and **12a** ($IC_{50} \geq 100$ and 44 μM for eqBuChE) were weaker inhibitors than **2b** ($IC_{50} = 35.5$ μM for eqBuChE) despite the better binding energies. However, at a relativistic level, some key correlations are evident; for example, in the case of **3b**, it was found to be more selective against BuChE and this is reflected in the binding energies for the (*S*)-enantiopode. The fact that human sequences are used for the docking and non-human for the bioassays might explain these divergences.

As regards the key atomic interactions (see Table s.1, SI), it is apparent that some of the inhibitors are better embedded in the enzyme active site than others. For instance, (*S*)-**12a**, (*S*)-**3f**, (*S*)-**3b**, (*S*)-**2b** and (*S*)-**2a**, stick out of the enzyme gorge to a certain extent and this possibly has an effect on the ligand binding.

Analysis of the crossdock graphic, shows key regular interactions between the ligand and the enzyme residues. For instance, a key interaction between the 2-carbonyl unit and Phe-295 is observed for (*R*)-**2a** and AChE and Trp-82 (part of the catalytic active site) with the benzene back-bone – probably via π-π interactions - of the same enantiomer in the

Table 4
Docking study of selected compounds against *h*AChE and *h*BuChE.

Inhibitor	AChE; Docking score (kcal/mol)	BuChE; Docking score (kcal/mol)
(*R*)-**2a**	−10.6	−6.3
(*R*)-**2b**	−8.0	−7.5
(*S*)-**2b**	−8.6	−6.5
(*R*)-**2c**	−8.0	−7.5
(*S*)-**2c**	−9.7	−6.5
(*S*)-**3b**	−3.5	−7.4
(*R*)-**3f**	−8.4	−5.9
(*S*)-**3f**	−5.8	−6.4
(*R*)-**12a**	−5.8	−11.4
(*S*)-**12a**	−11.80	−10.1

n.d = Not determined.

case of BuChE. This unit is also indicated in other inhibitor BuChE interactions like in the case of (*S*)-**2b,** (*S*)-**3b**, (*R*)-**3f** and (*R*)-**12a**. In fact, this latter inhibitor is embedded very well in the cavity of this enzyme.

Other interesting observations, are key interactions of the Phe295 unit of AChE and the Br in (*S*)-**2b**, Trp286 (AChE) with the benzene backbone of (*R*)-**2c** and (*S*)-**3b**.

Analysis of Table 3, show that the order of activity for BuChE inhibition is **3b** > **2b** > **12a**. Observation of the cross-dock diagrams confirms that all the inhibitors are reasonably embedded into the enzyme active site, with perhaps (*S*)-**3b** showing the best fit and (*R*)-**12a** a more looser binding confirmation.

The fact that single enantiomers were used for the docking, and only racemic mixtures for the bioassay studies might be the reason for discrepancies in the docking score values (which are generally good) and the moderate inhibitions observed.

3.7. *In silico drug-likeness and physicochemical properties*

We also carried out some *in silico* drug-likeness simulations using the SwissADME platform.[34,35] All the tested molecules are small-molecules with molecular weights in the range 250–500 g/mol. Most of these compounds showed Topological Polar Surface Areas (TPSA) between 40 and 56 Å^2, except for the nitro-containing molecules with TPSAs in the region 86–92 Å^2 and unfortunately these compounds were predicted to have no Blood Brain Barrier (BBB) permeability an issue which will need to be addresed in the design of future analogues. Compound **11c** is the only compound that breaks the Lipinski rule of five[36] Overall, this study showed that most of the compounds have good drug-likeness properties.

4. Conclusions

We successfully developed a synthetic strategy to access new oxindole derivatives, which was based on an efficient Indium mediated Barbier reaction. These compounds were tested against BACE1 and cholinesterases. Some of the compounds exhibited moderate BACE-1 inhibitions. In particular, compound **12a** exhibited promising results as a BACE1 inhibitor, achieving an inhibition percentage of almost 20 % at 10 μM. Additionally, our studies allowed us to tentatively consider the *S*-enantiomer as the eutomer (based on molecular docking), making the separation of its enantiomers a key goal for future work.

Regarding cholinesterase inhibition, five of the compounds gave moderate IC_{50} values in the case of BuChE (**2b**, **3a**, **3b**, **3d** and **12a**). However, **12a** was active against *ee*AChE with an IC_{50} of 68.5 μM. Among them, 1,3-diallyl-5-bromo-2-oxoindolin-3-yl **3b** demonstrated the best results, with an IC_{50} value of 23.8 μM and a mixed-type inhibition mechanism, allowing it to bind both to the free enzyme or the enzyme-substrate complex with moderate affinity.

As regards the question of dual inhibition, four of the inhibitors were shown to be weak inhibitors, (**3a**, **3b**, **3d** and **12a**). Work is continuing on the development of further analogues with better activities, including macrocyclic variants based on the oxindole scaffold.

CRediT authorship contribution statement

Catarina A. Montargil: Writing – original draft, Methodology, Investigation, Data curation. **Mariana Pinto:** Methodology, Investigation. **Rosa Resende:** Supervision, Methodology, Investigation, Formal analysis, Data curation. **Elisabete P. Carreiro:** Validation, Methodology, Investigation. **Alfonso T. García-Sosa:** Methodology, Formal analysis, Data curation. **Armanda E. Santos:** Writing – review & editing, Validation, Supervision, Resources, Formal analysis. **Anthony J. Burke:** Writing – review & editing, Writing – original draft, Visualization, Validation, Supervision, Resources, Project administration, Investigation, Funding acquisition, Formal analysis, Conceptualization.

Declaration of competing interest

The authors declare that they have no known competing financial interests or personal relationships that could have appeared to influence the work reported in this paper.

Acknowledgements

We acknowledge FCT (Portugal) for funding through the strategic project UIDB/00313/2020 | UIDP/00313/2020 to Coimbra Chemistry Centre – Institute of Molecular Sciences (CQC IMS) and to LAQV-REQUIMTE through the project UIDB/500026/2020 | UIDP/50006/2020. COMPETE 2020 - Operational Programme for Competitiveness and Internationalization and Portuguese national funds via FCT – Fundação para a Ciência e a Tecnologia, under projects UIDB/04539/2020, UIDP/04539/2020 and LA/P/0058/2020. ATG-S thanks the Estonian Research Council, for grant PRG1509. Rosa Resende is Post-Doctoral researcher (doi: 10.54499/DL57/2016/CP1448/CT0012). We acknowledge the UC-NMR facility for the NMR spectroscopic data (www.nmrccc.uc.pt) and particularly Mr. Pedro Cruz. We thank Dr. César Alberto Raposo (University of Salamanca) for all the help and support with the mass spectrometry. We are very grateful to Dr. Oksana Lockridge (University of Nebraska Medical Center, USA) for providing *h*BuChE.

Appendix A. Supplementary data

Supplementary data to this article can be found online at https://doi.org/10.1016/j.bmc.2025.118419.

Data availability

A data availability statement (DAS) is required to be submitted alongside all articles. Please read our full guidance on data availability statements for more details and examples of suitable statements you can use.

References

1.. World Alzheimer Report. *The Global Impact of Dementia: An Analysis of Prevalence, Incidence, Cost and Trends*. 2015.
2.. *Alzheimer's dementia.* Alzheimer Europe. https://www.alzheimer-europe.org/dementia/alzheimers-dementia (accessed 2024-06-13.
3.. 2023 Alzheimer's Disease Facts and Figures. *Alzheimers Dement.* 2023;19(4):1598–1695. https://doi.org/10.1002/alz.13016.
4.. Ghosh AK, Tang J. Prospects of β-secretase inhibitors for the treatment of Alzheimer's disease. *ChemMedChem*. 2015;10:1463–1466. https://doi.org/10.1002/cmdc.201500216.
5.. Jeppsson F, Eketjäll S, Janson J, et al. Discovery of AZD3839, a potent and selective BACE1 Inhibitor clinical candidate for the treatment of Alzheimer disease. *J Biol Chem.* 2012;287:41245–41257. https://doi.org/10.1074/sbcM112.409110.
6.. Coimbra JRM, Marques DFF, Baptista SJ, et al. Highlights in BACE1 inhibitors for Alzheimer's treatment. *Front Chem*. 2018;6(178). https://doi.org/10.3389/fchem.2018.00178.
7.. McDade E, Voytyuk I, Aisen P, et al. The case for low-level BACE1 inhibition for the prevention of Alzheimer disease. *Nat Rev Neurol*. 2021;17:703–714. https://doi.org/10.1038/s41582-021-00545-1.
8.. Zhang X-X, Tian Y, Wang Z-T, Ma Y-H, Tan L, Yu J-T. The epidemiology of Alzheimer's disease modifiable risk factors and prevention. *J Prev Alz Dis*. 2021:1–9. https://doi.org/10.14283/jpad.2021.15.
9.. Lane RM, Potkin SG, Enz A. Targeting acetylcholinesterase and Butyrylcholinesterase in dementia. *Int J Neuropsychopharmacol.* 2006;9(1):101–124. https://doi.org/10.1017/S1461145705005833.
10.. Rosenberry TL, Brazzolotto X, Macdonald IR, et al. Comparison of the binding of reversible inhibitors to human Butyrylcholinesterase and acetylcholinesterase: A crystallographic, Kinetic and Calorimetric Study. *Molecules*. 2017;22:2098. https://doi.org/10.3390/molecules22122098.
11.. Marques CS, López Ó, Bagetta D, et al. N-1,2,3-Triazole-Isatin derivatives for cholinesterase and β-amyloid aggregation inhibition: A comprehensive bioassay study. *Bioorg Chem.* 2020;98, 103753. https://doi.org/10.1016/j.bioorg.2020.103753.
12.. Bacalhau P, San Juan AA, Goth A, Caldeira AT, Martins R, Burke AJ. Insights into (S)-Rivastigmine inhibition of Butyrylcholinesterase (BuChE): molecular docking

and saturation transfer difference NMR (STD-NMR). *Bioorg Chem*. 2016;67: 105–109. https://doi.org/10.1016/j.bioorg.2016.06.002.
13.. Brandão P, López Ó, Leitzbach L, et al. Ugi Reaction Synthesis of Oxindole–Lactam Hybrids as Selective Butyrylcholinesterase Inhibitors. *ACS Med Chem Lett*. 2021;12 (11):1718–1725. https://doi.org/10.1021/acsmedchemlett.1c00344.
14.. Proschak E, Stark H, Merk D. Polypharmacology by design: A medicinal chemist's perspective on multitargeting compounds. *J Med Chem*. 2019;62:420–444. https://doi.org/10.1021/acs.jmedchem.8b00760.
15.. Totobenazara J, Bacalhau P, San Juan AA, et al. Synthesis and bioassays of 3-Substituted-3-Hydroxyoxindoles: donepezil analogues for cholinesterase inhibition. *ChemistrySelect*. 2016;1:3580–3588. https://doi.org/10.1002/slct.201600932.
16.. Marques CS, López Ó, Leitzbach L, Fernández-Bolaños JG, Stark H, Burke AJ. Survey of new, small-molecule Isatin-based Oxindole hybrids as multi-targeted drugs for the treatment of Alzheimer's disease. *Synthesis (Germany)*. 2022;54(19): 4304–4319. https://doi.org/10.1055/s-0041-1737343.
17.. Marques CS, McArdle P, Erxleben A, Burke AJ. Accessing new 5-α-(3,3 Disubstituted Oxindole)-Benzylamine derivatives from Isatin: Stereoselective Organocatalytic three component Petasis reaction. *Eur J Org Chem*. 2020;2020(24): 3622–3634. https://doi.org/10.1002/ejoc.202000334.
18.. Marques CS, Burke AJ. Enantioselective rhodium(I)-catalyzed additions of Arylboronic acids to N-1,2,3-Triazole-Isatin derivatives: accessing N-(1,2,3-Triazolmethyl) 3-Hydroxy-3-Aryloxindoles. *ChemCatChem*. 2016;8(22):3518–3526. https://doi.org/10.1002/cctc.201600901.
19.. Hofmanova T, Marques C, García-Sosa AT, et al. N-substituted 3-Aminooxindoles and N-Propargyl derivatives: potential biological activities against Alzheimer's disease. *Res Chem*. 2023;6, 101032. https://doi.org/10.1016/j.rechem.2023.101032.
20.. Gong JH, Lee KY, Son JS, Kim JN. Indium mediated Barbier reaction of Ninhydrin and Isatin. *Bull Korean Chem Soc*. 2003;24(4):507–510. https://doi.org/10.5012/BKCS.2003.24.4.507.
21.. Rajeshkumar V, Chandrasekar S, Sekar G. An Efficient Route to Synthesize Isatins by Metal-Free, Iodine-Catalyzed Sequential C(Sp^3)–H Oxidation and Intramolecular C–N Bond Formation of 2′-Aminoacetophenones. *Org Biomol Chem*. 2014;12(42): 8512–8518. https://doi.org/10.1039/C4OB01564A.
22.. Anbu N, Nagarjun N, Jacob M, Kalaiarasi JMVK, Dhakshinamoorthy A. Acetylation of alcohols, amines, phenols, thiols under catalyst and solvent-free conditions. *Chemistry*. 2019;1(1):69–79. https://doi.org/10.3390/chemistry1010006.
23.. Garden SJ, Torres JC, Da Silva LE, Pinto AC. A convenient methodology for the N-alkylation of Isatin compounds. *Synth Commun*. 1998;28(9):1679–1689. https://doi.org/10.1080/00397919808006872.
24.. García-Sosa AT, Mancera RL, Dean PM. WaterScore: A Novel method for distinguishing between bound and displaceable water molecules in the crystal structure of the binding site of protein-ligand complexes. *J Mol Model*. 2003;9(3): 172–182. https://doi.org/10.1007/s00894-003-0129-x.
25.. García-Sosa AT, Sild S, Maran U. Docking and virtual screening using distributed grid technology. *QSAR Comb Sci*. 2009;28(8):815–821. https://doi.org/10.1002/qsar.200810174.
26.. (a) García-Sosa AT. Hydration properties of ligands and drugs in protein binding sites: tightly-bound, bridging water molecules and their effects and consequences on molecular design strategies. *J Chem Inf Model*. 2013;53(6):1388–1405. https://doi.org/10.1021/ci3005786.(b)Stevanovic, S.; Sencanski, M.; Danel, M.; Menendez, C.; Belguedj, R.; Bouraiou, A.; Nikolic, K.; Cojean, S.; Loiseau, P.M.; Glisic, S.; et al. Synthesis, in silico, and in vitro evaluation of anti-leishmanial activity of Oxadiazoles and Indolizine containing compounds flagged against anti-targets. Molecules 2019, 24, 1282. https://doi.org/10.3390/molecules24071282.
27.. Fernandes T, Resende R, Silva DF, et al. Structural and functional alterations in mitochondria-associated membranes (MAMs) and in mitochondria activate stress response mechanisms in an in vitro model of Alzheimer's disease. *Biomedicines*. 2021;9(8):881. https://doi.org/10.3390/biomedicines9080881.
28.. Resende R, Ferreira-Marques M, Moreira P, et al. New BACE1 chimeric peptide inhibitors selectively prevent AβPP-β cleavage decreasing amyloid-β production and accumulation in Alzheimer's disease models. *J Alzheimer's Dis*. 2020;76(4): 1317–1337. https://doi.org/10.3233/JAD-200381.
29.. Fonseca ACRG, Proença T, Resende R, Oliveira CR, Pereira CMF. Neuroprotective effects of statins in an in vitro model of Alzheimer's disease. *J Alzheimer's Dis*. 2009; 17(3):503–517. https://doi.org/10.3233/JAD-2009-1067.
30.. Ghosh AK, Osswald HL. BACE1 (beta-secretase) inhibitors for the treatment of Alzheimer's disease. *Chem Soc Rev*. 2014;43:6765–6813. https://doi.org/10.1039/c3cs60460h.
31.. Patrick GL. *An Introduction to Medicinal Chemistry*. 6th ed. Oxford University Press; 2017.
32.. Eketjäll S, Jansona J, Kasperssonc K, et al. AZD3293: A Novel, Orally Active BACE1 Inhibitor with High Potency and Permeability and Markedly Slow Off-Rate Kinetics. *J Alzheimer's Dis*. 2016;50:1109–1123. https://doi.org/10.3233/JAD-150834.
33.. Denizot F, Lang R. Rapid colorimetric assay for cell growth and survival. *J Immunol Methods*. 1986;89(2):271–277. https://doi.org/10.1016/0022-1759(86)90368-6.
34. Daina A, Michielin O, Zoete V. SwissADME: a free web tool to evaluate pharmacokinetics, drug-likeness and medicinal chemistry friendliness of small molecules. *Sci Rep*. 2017;7, 42717. https://doi.org/10.1038/srep42717.
35.. Montargil C. *MSc Dissertation*. University of Coimbra; 2024.
36.. Lipinski CA, Lombardo F, Dominy BW, Feeney PJ. Experimental and computational approaches to estimate solubility and permeability in drug discovery and development settings. *Adv Drug Deliv Rev*. 1997;23:3–25. https://doi.org/10.1016/S0169-409X(96)00423-1) rule.).